

**FACULDADE DE ENGENHARIA DA UNIVERSIDADE DO PORTO**

# **Augmented Reality Tools applied to Alzheimer's Disease Research**

**Nuno André Brandão Costa Neves**



**FEUP** FACULDADE DE ENGENHARIA  
UNIVERSIDADE DO PORTO

Mestrado Integrado em Bioengenharia

Supervisor: Prof. Dr. Pedro Martins

June 28, 2020

© Nuno A.B.C. Neves, 2020

# **Augmented Reality Tools applied to Alzheimer's Disease Research**

**Nuno André Brandão Costa Neves**

Mestrado Integrado em Bioengenharia



**This thesis was supervised by:**

Professor Pedro Alexandre Lopes de Sousa Martins (supervisor)

INEGI - Instituto de Ciência e Inovação em Engenharia Mecânica e Engenharia Industrial,  
Portugal

FEUP - Faculdade de Engenharia da Universidade do Porto, Portugal

**Institution where this dissertation was performed:**

INEGI - Instituto de Ciência e Inovação em Engenharia Mecânica e Engenharia Industrial,  
Portugal



# Resumo

Realidade virtual (VR) é uma tecnologia utilizada atualmente em variados setores da indústria devido ao seu elevado número de aplicações. No entanto, o ambiente virtual (VE) originado pelo sistema de VR carece de interação adequada com o mundo real. Dado que todo este ambiente é criado virtualmente pelo programador, não há interação com o verdadeiro ambiente circundante do utilizador. Como possível solução para este problema, a realidade aumentada foi criada para unir os mundos virtual e real.

Tal como a realidade virtual, a realidade aumentada permite infinitas aplicações. Contudo, dado que esta tecnologia é relativamente recente, não há muitas soluções implementadas e usadas pela indústria. Consequentemente, esta é uma tecnologia com espaço para melhorar e crescer, tornando a ideia de a trabalhar e desenvolver extremamente interessante.

A realidade aumentada tem vindo a ser estudada pelo projeto NorthStar, que utiliza o sensor Leap Motion para realizar rastreamento das mãos. Sendo este um projeto de código aberto, este foi o ponto de início para o desenvolvimento do sistema de realidade aumentada da dissertação. De forma a aumentar a imersão do utilizador no sistema de realidade aumentada, o sensor Structure Core foi introduzido para adquirir percepção de profundidade.

O Alzheimer é um doença neurodegenerativa que afeta as células cerebrais, conduzindo a uma diminuição da função cognitiva. A maioria dos estudos sobre este tema são focados na análise da espessura cortical cerebral, que pode ser adquirida através de imagens de ressonância magnética (MRI). Este estudo tem como alvo o desenvolvimento de ferramentas de realidade aumentada para auxiliar a pesquisa sobre a doença de Alzheimer, através da investigação das diferenças em espessura cortical em grupos distintos de sujeitos (cognitivamente normal, preocupação significativa de memória, dano cognitivo leve, doença de Alzheimer), usando a base de dados Alzheimer's Disease Neuroimaging Initiative (ADNI). Os MRI's da base de dados foram processados com Freesurfer, um software que permite gerar medidas da espessura cortical para diferentes regiões cerebrais.

Os resultados foram representados num modelo cerebral 3D na forma de um gradiente de cores, sendo estas proporcionais à perda de espessura cortical registada para cada região do cérebro. Para a avaliação da eficiência da tecnologia, os resultados foram comparados com estudos de referência no âmbito da doença de Alzheimer. Tal demonstra que os métodos utilizados nesta dissertação são eficientes e representam uma alternativa na investigação da doença.

**Palavras-chave:** Realidade Virtual, Realidade Aumentada, Leap Motion, Structure Core, Doença de Alzheimer, Espessura Cortical



# Abstract

Virtual reality is a technology currently being used in many industry sectors, due to its high number of applications. However, the virtual environment originated from the virtual reality system lacks a proper interaction with the real-world. Since all the environment is created virtually by a developer, there's no interaction with the user's real surroundings. As a possible solution for this issue augmented reality has been created to unite the virtual-world with the real-world.

Like virtual reality, augmented reality can be used with infinite applications. However, since the tech is relatively new, there are not many applications already implemented and used by the industry. Hence, it is a technology with room to improve, which makes the idea of working and developing it more interesting.

Augmented reality is being studied by project NorthStar, which uses the Leap Motion sensor to acquire hand tracking. Since the project is open-sourced, this was the beginning point for the development of the augmented reality system for the dissertation. To increase the immersion of the user into the augmented reality system, the Structure Core sensor was implemented to acquire depth perception.

Alzheimer's disease is a neurodegenerative impairment which affects the brain cells leading to a decrease of cognitive function. The majority of the studies around this subject are focused on the brain cortical thickness analysis, which can be acquired through magnetic resonance imaging (MRI). This study aims the development of augmented reality tools to aid the alzheimer's disease research by exploring the differences in cortical thickness of distinct cohort subjects (cognitively normal, significant memory concern, mild cognitive impairment, alzheimer's disease) using the Alzheimer's Disease Neuroimaging Initiative (ADNI) database. The MRI's from the database were processed with FreeSurfer, which generated cortical thickness measures for different brain regions.

The results were represented in a 3D brain model as a gradient of colors, with the colors being proportional to the loss of cortical thickness registered for each brain region. In order to evaluate the efficiency of the technology, the results were compared to reference studies in alzheimer's disease research. This demonstrates that the methods used in this dissertation are efficient and represent an alternative perspective for alzheimer's disease research.

**Keywords:** Virtual Reality, Augmented Reality, Leap Motion, Structure Core, Alzheimer's Disease, Cortical Thickness



# Acknowledgements

I would like to gracefully acknowledge the individuals who assisted me in the research and development of this dissertation. Firstly, my supervisor Prof. Dr. Pedro Martins for his valuable inputs, guidance and availability and Sérgio Pinto for mentoring and introducing me to this subject.

Data collection and sharing for this project was funded by the Alzheimer's Disease Neuroimaging Initiative (ADNI) (National Institutes of Health Grant U01 AG024904) and DOD ADNI (Department of Defense award number W81XWH-12-2-0012). ADNI is funded by the National Institute on Aging, the National Institute of Biomedical Imaging and Bioengineering, and through generous contributions from the following: AbbVie, Alzheimer's Association; Alzheimer's Drug Discovery Foundation; Araclon Biotech; BioClinica, Inc.; Biogen; Bristol-Myers Squibb Company; CereSpir, Inc.; Cogstate; Eisai Inc.; Elan Pharmaceuticals, Inc.; Eli Lilly and Company; EuroImmun; F. Hoffmann-La Roche Ltd and its affiliated company Genentech, Inc.; Fujirebio; GE Healthcare; IXICO Ltd.; Janssen Alzheimer Immunotherapy Research & Development, LLC.; Johnson & Johnson Pharmaceutical Research & Development LLC.; Lumosity; Lundbeck; Merck & Co., Inc.; Meso Scale Diagnostics, LLC.; NeuroRx Research; Neurotrack Technologies; Novartis Pharmaceuticals Corporation; Pfizer Inc.; Piramal Imaging; Servier; Takeda Pharmaceutical Company; and Transition Therapeutics. The Canadian Institutes of Health Research is providing funds to support ADNI clinical sites in Canada. Private sector contributions are facilitated by the Foundation for the National Institutes of Health ([www.fnih.org](http://www.fnih.org)). The grantee organization is the Northern California Institute for Research and Education, and the study is coordinated by the Alzheimer's Therapeutic Research Institute at the University of Southern California. ADNI data are disseminated by the Laboratory for Neuro Imaging at the University of Southern California.

I would like to also acknowledge my parents, brother and family for their continued support, love, sacrifice and encouragement, for always giving me access to the best education and providing for my times at UTAD, FEUP and Karolinska Institutet. My group of friends and Rafaela for their friendship, patience, sense of humor and constant words of encouragement. Finally, my thanks go to all the people who have supported me to complete this work directly or indirectly.

Nuno Neves



*“Logic will get you from A to B,  
Imagination will take you everywhere.”*

Albert Einstein



# Contents

|          |   |           |
|----------|---|-----------|
| <b>1</b> | <b>Introduction</b>                                     | <b>1</b>  |
| 1.1      | Context . . . . .                                       | 1         |
| 1.2      | Motivation . . . . .                                    | 2         |
| 1.3      | Aim of the work . . . . .                               | 2         |
| 1.4      | Structure . . . . .                                     | 3         |
| <b>2</b> | <b>Technical &amp; Theoretical Background</b>           | <b>5</b>  |
| 2.1      | Depth Perception . . . . .                              | 5         |
| 2.1.1    | Stereopsis . . . . .                                    | 5         |
| 2.1.2    | LiDAR . . . . .   | 7         |
| 2.2      | Sensor Descriptions . . . . .                           | 8         |
| 2.2.1    | Stereo Camera . . . . .                                 | 8         |
| 2.2.2    | Time of Flight . . . . .                                | 9         |
| 2.2.3    | Structured Light Depth Sensor . . . . .                 | 9         |
| 2.3      | Summary . . . . .                                       | 10        |
| <b>3</b> | <b>Virtual Reality &amp; Augmented Reality</b>          | <b>11</b> |
| 3.1      | Virtual Reality . . . . .                               | 11        |
| 3.1.1    | Virtual Reality Definition . . . . .                    | 11        |
| 3.1.2    | The History of Virtual Reality . . . . .                | 12        |
| 3.1.3    | Virtual Reality Applications . . . . .                  | 14        |
| 3.2      | Augmented Reality: a new way to see the world . . . . . | 17        |
| 3.2.1    | The History of Augmented Reality . . . . .              | 18        |
| 3.2.2    | Augmented Reality Application . . . . .                 | 19        |
| 3.2.3    | Augmented Reality of Today . . . . .                    | 21        |
| 3.2.4    | UltraLeap: Leap Motion Sensor . . . . .                 | 22        |
| 3.2.5    | Project NorthStar . . . . .                             | 22        |
| <b>4</b> | <b>Alzheimer's Disease</b>                              | <b>25</b> |
| 4.1      | Neurodegenerative Disease . . . . .                     | 25        |
| 4.2      | Investigating AD . . . . .                              | 26        |
| 4.2.1    | ADNI Database . . . . .                                 | 26        |
| 4.2.2    | Desikan-Killiany Brain Atlas . . . . .                  | 28        |
| 4.3      | Conclusion . . . . .                                    | 30        |
| <b>5</b> | <b>Methods I: Hardware Implementation</b>               | <b>31</b> |
| 5.1      | Calibration . . . . .                                   | 32        |
| 5.1.1    | Leap Motion . . . . .                                   | 32        |

|                   |   |           |
|-------------------|---|-----------|
| 5.1.2             | Headset lens . . . . .  | 32        |
| 5.2               | Structure Core . . . . .  | 32        |
| 5.2.1             | Sensor: Structure by Occipital . . . . .  | 33        |
| 5.2.2             | Structure Core in detail . . . . .  | 33        |
| 5.2.3             | Sensor Implementation . . . . .   | 34        |
| <b>6</b>          | <b>Methods II: AR &amp; 3D Models</b>   | <b>35</b> |
| 6.1               | AR Development . . . . .  | 35        |
| 6.2               | 3D Models . . . . .   | 36        |
| 6.2.1             | Models Application . . . . .  | 37        |
| 6.3               | 3D Model Manipulation in AR . . . . .   | 38        |
| 6.3.1             | Model Selection Menu . . . . .  | 38        |
| <b>7</b>          | <b>Methods III: AR for Alzheimer Disease Study</b>                                | <b>41</b> |
| 7.1               | Proof of Concept . . . . .  | 41        |
| 7.1.1             | ADNI Cortical Thickness Data . . . . .  | 41        |
| 7.1.2             | 1 <sup>st</sup> Study - ADNI Statistical Analysis . . . . .                       | 42        |
| 7.1.3             | 2 <sup>nd</sup> Study - AR Representation of Cortical Thickness Results . . . . . | 43        |
| 7.2               | AR development for AD study . . . . .   | 44        |
| 7.2.1             | Stages Menu . . . . .   | 44        |
| 7.2.2             | Loss Bar . . . . .  | 44        |
| 7.2.3             | AR system . . . . .   | 45        |
| <b>8</b>          | <b>Results &amp; Discussion</b>   | <b>47</b> |
| 8.1               | 1 <sup>st</sup> Study - ADNI Statistical Analysis . . . . .                       | 47        |
| 8.2               | 2 <sup>nd</sup> Study - AR Representation of Cortical Thickness Results . . . . . | 50        |
| 8.3               | Discussion . . . . .  | 52        |
| <b>9</b>          | <b>Conclusions</b>  | <b>55</b> |
| <b>10</b>         | <b>Future Work</b>  | <b>57</b> |
| <b>References</b> |   | <b>59</b> |
| <b>A</b>          | <b>Recorded Videos</b>  | <b>67</b> |
| <b>B</b>          | <b>Tables - Chapter 8</b>   | <b>69</b> |

# List of Figures

|      |  |    |
|------|--|----|
| 2.1  | Geometry of binocular stereopsis. An objects' depth is perceived with relative to the fixation point. As the object comes toward the fixation point, angular disparity is reduced. Angular disparity is proportional to the depth perceived with relative to point P [11]. . . . . | 6  |
| 2.2  | LiDAR's terrain mapping [14]. . . . .  | 8  |
| 3.1  | Brain Sensory Stimulation's. . . . .   | 12 |
| 3.2  | The CAVE at Electronic Visualization Laboratory, University of Illinois at Chicago [32]. . . . .   | 13 |
| 3.3  | Driving Simulator [34]. . . . .  | 14 |
| 3.4  | Cockpit of a flight simulator [35]. . . . .  | 14 |
| 3.5  | Reality-virtuality Continuum [42] [4]. . . . .   | 17 |
| 3.6  | User wearing the MARS prototype [46]. . . . .  | 18 |
| 3.7  | a) Head-mounted display prototype [53]; b) Remote user representation in the AR interface [47]; c) View of volume rendered fetus within pregnant subject [50]. . . . .   | 20 |
| 3.8  | Scheme of the AR basic system. . . . .   | 21 |
| 3.9  | Leap Motion device. . . . .  | 22 |
| 3.10 | Headset Parts. . . . .   | 23 |
| 4.1  | ADNI based patient MRI's. . . . .  | 27 |
| 4.2  | Desikan-Killiany Brain Atlas. . . . .  | 29 |
| 5.1  | 3 main components of the work. . . . .   | 31 |
| 5.2  | a) Leap Motion Controller Calibration; b) Lens Calibration Toolbox. . . . .  | 32 |
| 5.3  | Structure Core Hardware Architecture [75]. . . . .   | 33 |
| 5.4  | Headset with SC and Leap Motion sensors. . . . .   | 34 |
| 6.1  | AR virtual hands representation in Unity. . . . .  | 36 |
| 6.2  | Skull model different views: a) Front b) Back c) Left side d) Right side. . . . .  | 37 |
| 6.3  | Brain model different views: a) Front b) Back c) Left side d) Right side. . . . .  | 37 |
| 6.4  | Representation of the model rotation/selection menu. . . . .   | 38 |
| 7.1  | Disease stages menu. . . . .   | 44 |
| 7.2  | Loss bar. . . . .  | 44 |
| 7.3  | a) Model with On/Off button b) Disease menu c) Disease stages menu d) Loss bar. . . . .  | 45 |
| 8.1  | AD analysis with temporal and parietal lobes marked: a) Left view b) Right view. . . . .   | 52 |
| 8.2  | Entorhinal ROI for a) MCI analysis b) AD analysis. . . . .   | 52 |



# List of Tables

|     |   |    |
|-----|---|----|
| 2.1 | 3 Types Comparison . . . . .  | 10 |
| 3.1 | Teleoperation Applications . . . . .  | 16 |
| 3.2 | Figure 3.10 Label . . . . .   | 24 |
| 4.1 | Figure 4.2 Label . . . . .  | 29 |
| 7.1 | ADNI Subject Characteristics . . . . .  | 42 |
| 8.1 | Mean differences between the CN group and the other 3 cohorts (millimeters) . . . . . | 48 |
| 8.2 | Mean differences (%) between the CN group and the other 3 cohorts . . . . .           | 49 |
| 8.3 | Cortical thickness results for the three cohorts . . . . .                            | 51 |
| B.1 | Cortical thickness in CN group (mean and standard deviation, millimeters) . . . . .   | 70 |
| B.2 | Cortical thickness in SMC group (mean and standard deviation, millimeters) . . . . .  | 71 |
| B.3 | Cortical thickness in MCI group (mean and standard deviation, millimeters) . . . . .  | 72 |
| B.4 | Cortical thickness in AD group (mean and standard deviation, millimeters) . . . . .   | 73 |



# Abbreviations

|       |   |
|-------|---|
| AD    | Alzheimer's Disease                         |
| ADNI  | Alzheimer's Disease Neuroimaging Initiative |
| ApoE  | Apolipoprotein E                            |
| AR    | Augmented Reality                           |
| CAVE  | Cave Automatic Virtual Environment          |
| CCD   | Charge-Coupled Device                       |
| CN    | Cognitively Normal                          |
| CSF   | Cerebrospinal Fluid                         |
| DOF   | Degrees of Freedom                          |
| GO    | Game Object                                 |
| GPS   | Global Positioning System                   |
| HMD   | Head-Mounted Display                        |
| HUD   | Heads Up Display                            |
| LCD   | Liquid-Crystal Display                      |
| LED   | Light-Emitting Diode                        |
| LiDAR | Light Detection And Ranging                 |
| MARS  | Mobile Augmented Reality System             |
| MCI   | Mild Cognitive Impairment                   |
| MRI   | Magnetic Resonance Imaging                  |
| NS    | NorthStar                                   |
| PMMA  | Poly(Methyl Methacrylate)                   |
| RE    | Real Environment                            |
| ROI   | Region of Interest                          |
| SC    | Structure Core                              |
| SL    | Structured Light                            |
| SMC   | Significant Memory Concern                  |
| ToF   | Time of Flight                              |
| VE    | Virtual Environment                         |
| VR    | Virtual Reality                             |



# Chapter 1

## Introduction

This chapter introduces the general context of the work, alongside the motivation to accomplish the proposed objectives. The last section presents the chosen structure for the dissertation.

### 1.1 Context

According to Jonathan Steuer *et al.* [1], Virtual Reality (VR) has reached the press community as a medium, which was a collection of technological hardware such as computers, head-mounted displays, and motion-sensing gloves.

The majority of the authors define virtual reality as an immersion of the user in a responsive virtual world, implying user dynamic control of viewpoint [2]. Besides the great advances in different areas of work, originated by VR applications, it is clear that the technology is lacking in real-world aspect. Since the user is completely immersive in the VR state, he is not aware of his real surroundings. Therefore, the real world needs to be an aspect to have in counter, in order to amplify the possible applications of this technology.

To solve the problem, Augmented Reality (AR) was introduced to the community. There are distinct opinions regarding the position of AR as a technology. Otherwise speaking, some authors such as Wilson [3], consider that AR is a form of application of VR, while other authors defend the idea of a ‘reality-virtuality continuum’ (figure 3.5) where AR is towards the real-world side of the continuum and VR is at the opposite extreme [4][5].

Alzheimer’s disease (AD) is a neurodegenerative impairment, that is caused by the neurodegeneration of brain tissue such as cell systems. According to Clifford R. Jacket al. [6], the neurodegeneration is caused by the abnormal processing of  $\beta$ -amyloid peptide, which will lead to atrophy of brain cortical thickness. The disease promotes deterioration in cognitive function and body behavior, and since it is a dementia with treatments that only delay the impairment, AD has been a theme of discussion for many neurodegenerative researchers worldwide. With that in mind

the Alzheimer's Disease Neuroimaging Initiative (ADNI)<sup>1</sup> was created to aid the AD research, since it is an available open-source MRI's database.

## 1.2 Motivation

*"Augmented Reality In Healthcare Will Be Revolutionary."* [7]

Recent studies indicate that AR can be a decisive technology for healthcare future advances. From improved surgery techniques to detailed displaying image methods, AR implementation can make the difference in a large window of potential applications.

According to Zion Market Research, in 2018 the global healthcare augmented and virtual reality market was evaluated in approximately €775 million and is expected to increase to €4,670 million by 2025. These numbers show the market expansion for this new technology, making AR & VR the leading solutions for patient care innovations. Another interesting aspect is the use of AR systems to develop and improve medical education [8].

Neurodegenerative related diseases are gaining some recognition in the science community, in specific AD. According to the Alzheimer's Association [9], it is estimated that in the United States 5.8 million people have lived with AD in 2019. Furthermore, with age being the predominant risk factor for the disease, and since average life expectancy is increasing, it is clear to conclude that AD incidence will increase over the years.

Nowadays, AD is a dementia that only can be delayed. For that reason, the objective of this work is to open a new perspective of research for the disease, with the creation of an AR tool.

## 1.3 Aim of the work

The concept of AR is something that can be measured by the interconnection between the real world and the virtual scenes developed by humans. Such knowledge opens many applications possibilities and depends only on the developer's imagination.

With the application of the technology to the biomedical engineering branch in sight, AD offers a reliable area of study. Since there is a previous disease knowledge, the implementation of the AR to the study of AD is facilitated.

The most important aim of the work is to develop a stable and balanced AR environment with data shared between a hand tracking device, and a depth analysis device in order to create an AR tool for AD research. Hence, the state of art is performed in order to know and understand in which stage are current AR projects, regarding the fact that the technology is relatively new for the scientific community. As mentioned earlier, due to the window of opportunities that AR creates,

---

<sup>1</sup>Data used in preparation of this article were obtained from the Alzheimer's Disease Neuroimaging Initiative (ADNI) database ([adni.loni.usc.edu](http://adni.loni.usc.edu)). As such, the investigators within the ADNI contributed to the design and implementation of ADNI and/or provided data but did not participate in analysis or writing of this report. A complete listing of ADNI investigators can be found at: [http://adni.loni.usc.edu/wp-content/uploads/how\\_to\\_apply/ADNI\\_Acknowledgement\\_List.pdf](http://adni.loni.usc.edu/wp-content/uploads/how_to_apply/ADNI_Acknowledgement_List.pdf)

there has been a lot of investment to acquire AR development knowledge since the beginning of the 21st century.

## 1.4 Structure

The remainder of the work is structured as follows: in chapter 2, the technical and theoretical depth perception background is represented, such as the description of some devices that can evaluate depth. Chapter 3 describes VR and AR with a brief history and applications, concluding with section 3.2.3, where today's developments of AR are presented, and the project NorthStar is introduced. The chapter 4 initializes with the presentation of the Alzheimer's Disease.

The methods component is divided into 3 chapters, chapter 5 explains the system calibration process and the implementation of the SC sensor. Chapter 6 describes the AR development environment, with the insertion of the 3D models and its manipulations. Finally, chapter 7 explores the AR development for the AD study and research, with the implementation of two studies. Chapter 8 reports the results and discussion.

Chapter 9 comprises a brief summary of the main conclusions of the work exposed and chapter 10 explores future lines of investigation regarding the same topics exposed in this dissertation.



# **Chapter 2**

## **Technical & Theoretical Background**

The significance of this chapter is to clarify the meaning and importance of the application of depth perception to the core of Virtual and Augmented Reality.

In order to understand that, it is a matter of great importance to analyze the role of depth perception to human life, explaining how humans can become aware of the objects distances in the surrounding environment.

### **2.1 Depth Perception**

When looking for the definition of depth perception, it's better to divide the two words. Depth means either the distance from the top to the bottom of something or the distance below the top surface. Perception is a process which involves the recognition and interpretation of different sensing stimulation's [10] acquired from distinct body sensors, which can lead to a unique response or a shared one. For that reason, depth perception is defined as the ability to analyze and comprehend the objects and the around environment in a 3 dimensional way, calculating the distance between objects in order to measure its location in the scheme.

Perception is processed in the human brain when the brain compares contrasting pictures from each eye and combines them to form a single 3D image. Stereopsis results from two images projected by the two eyes; human eyes are located at different lateral positions. Hence, the resulting images share some differences relative to the object's horizontal position. These differences are defined as binocular disparities.

#### **2.1.1 Stereopsis**

Binocular vision or stereopsis is an essential feature in order to have depth perception, and is obtained based on visual information deriving from the eyes. In other words, the fact that humans have the possibility of analyze the information from the different receptors in both eyes, unleashes the perception of the distance.

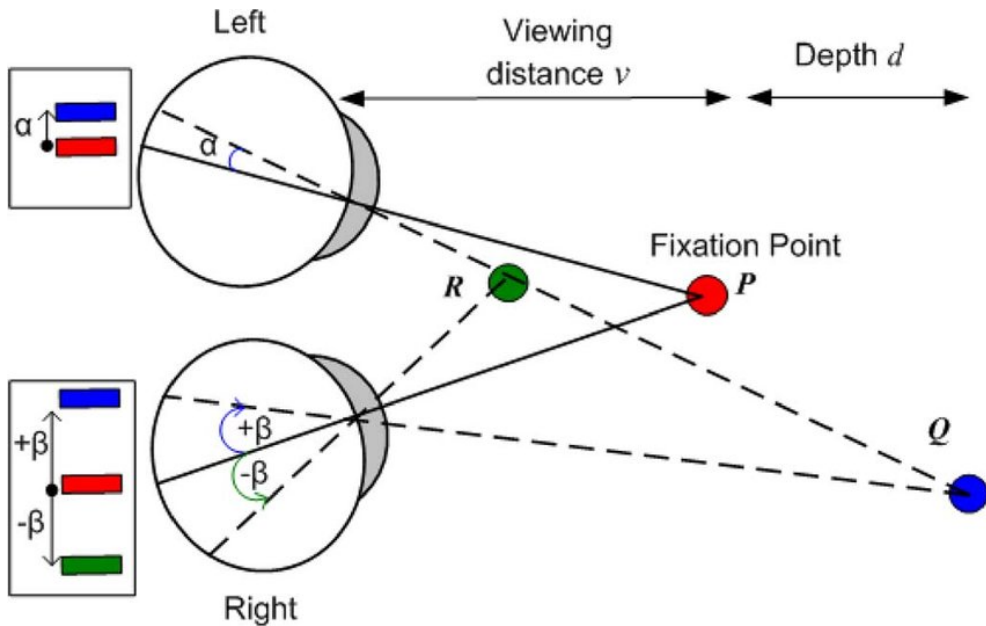


Figure 2.1: Geometry of binocular stereopsis. An objects' depth is perceived with relative to the fixation point. As the object comes toward the fixation point, angular disparity is reduced. Angular disparity is proportional to the depth perceived with relative to point P [11].

Stereopsis is processed in the visual cortex, more specifically in binocular cells that have different receptive fields in the horizontal positions in human eyes. In order to activate these cells, a stimulus needs to be in the correct position in the left and right eyes. This phenomenon is called disparity detector. If the human stares at an object, the two eyes converge, and that leads to a combination of the two created images in the center of the retina in both eyes. Then, because the human vision only can pin one object as center, the surrounding objects appear shifted in comparison to the centered object, and the binocular cells in the visual cortex give a depth value to the different shifted points that constitute the shifted objects.

Due to the lateral separation of the eyes, the disparity is mainly along the horizontal position defined by the interocular axis. The vertical position is usually much smaller. The disparity is defined as a two dimensional vector with some independent components. For the reason, the retinal surface of the eyes is 2D [12].

### 2.1.1.1 Mathematical Perception

In Figure 2.1, the process of binocular disparity is represented. Both eyes are represented having in sight the three points R, P and Q.

Point Q makes an  $\alpha$  angle with the left fovea, and a  $\beta$  angle with the right fovea. According to D. V.S.X. De Silva *et al.* [11], binocular disparity ( $\eta$ ) can be defined as  $(\beta - \alpha)$ , which represents an angular disparity of:

$$\eta Q = (\beta - \alpha) \quad (2.1)$$

The same can be applied for point R, with the angular disparity ( $\eta R$ ) being represented as:

$$\eta R = -(\beta + \alpha) \quad (2.2)$$

With equations 2.1 and 2.2 in mind, further conclusions can be made:  $\eta Q > 0$  and  $\eta R < 0$ .

Concluded the math calculations, the brain needs to understand the different equation's results. Using the angular disparities observed in points Q and R, the brain has the ability to recognize the depth position of point P in relation to the referred points. Taking this into consideration, when the  $\eta$  is greater than zero, the brain interprets that point Q is behind fixation point P. The opposite happens, when point R is considered, since the point's  $\eta$  is less than zero, which means that R is in front of fixation point P. Also, other information can be extracted, as claimed in [13]. Binocular disparity can be calculated by analysing the dependencies between depth value ( $d$ ) and viewing distance ( $v$ ).

$$\eta \approx \frac{d}{v^2} \quad (2.3)$$

Equation 2.3 contributes to the comprehension of the interactions between the different domains. Binocular disparity is directly proportional to the depth domain. On the other hand, binocular disparity has a faster reduction with the increase of the viewing distance. Notice that, with a large distance value increase, the binocular disparity values tends to be too small to be detected.

### 2.1.2 LiDAR

One example of the application of depth perception is the Light Detection And Ranging (LiDAR) method. LiDAR was created as a surveying method. Using ultraviolet, visible or near-infrared light, it can measure the distance to an object or a target by illuminating the object. The reflected light will be measured with a sensor, in order to calculate the disparity of distances of different objects in relation to the position where LiDAR stands. Differences in laser light return times and wavelengths are used to create the digital 3D model of the surrounding environment.

Initially, the LiDAR system was developed for military purposes, and, per example, in 1960, the system was applied to aircraft (LiDAR UK) with the function to detect enemy submarines, as the result of the invention of the laser back in the 1930s.

The majority of LiDAR systems have a unique laser that fires onto a rotating mirror, but there are other methods like the Velodyne that uses a rotating head with 64 semiconductors lasers, each one firing up to twenty-thousand times per second. With this new approach, Velodyne achieves data collection rates with a higher magnitude in comparison with the conventional LiDAR designs [15]. The LiDAR system, in general, is already being used by society in different areas such as in mobile robots (per example, agricultural robots for a variety of purposes, ranging from seed and fertilizer dispersions, sensing techniques, as well as crop scouting for the task of weed control), in archaeology including planning of field campaigns, mapping features under forest canopy, and overview of broad, continuous features indistinguishable from the ground (figure 2.2) [16]. LiDAR is being tested in autonomous vehicles for obstacle detection and avoidance to navigate

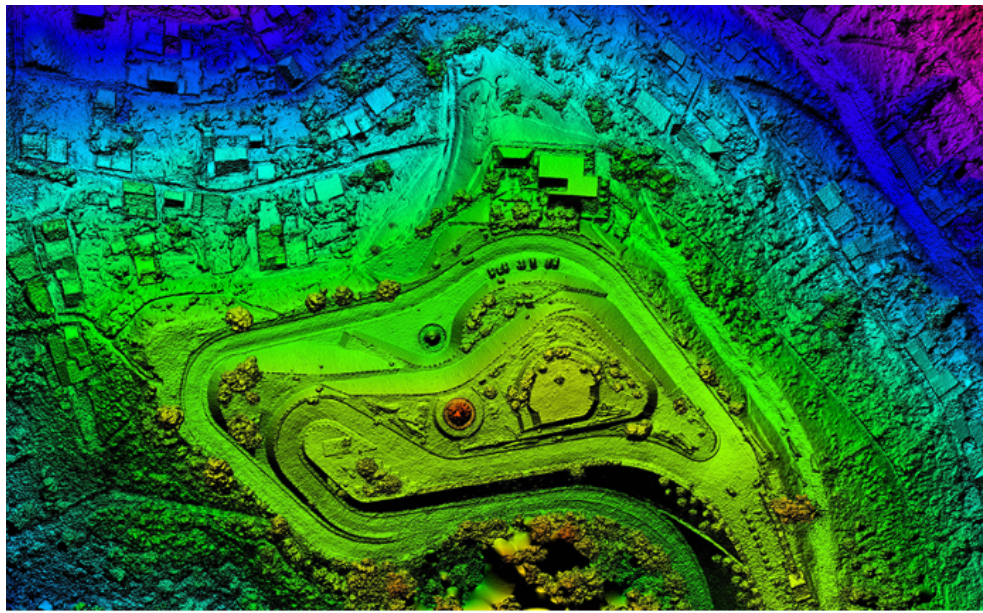


Figure 2.2: LiDAR's terrain mapping [14].

safely through environments [17]. Geomorphology is the most popular field that uses LiDAR, and is defined by the study of the evolution of the Earth's surface both on land and underwater, by looking at the topographic and bathymetric features that have been altered by physical or chemical processes.

Nowadays, it is accepted that LiDAR is irreplaceable when used in this area of study.

"device specifications must be selected carefully according to the objectives of the study" [18]

This sentence explains the important role of the LiDAR system in the evolution of some areas of study. This technology allows the combination between science and management to equate better decision-making ethics [19].

## 2.2 Sensor Descriptions

Besides the large scale application of depth perception presented before, this knowledge is also being applied to minor objects. Therefore, in this section, three distinct types of devices are described. From the stereo camera environment in addition to time of flight and structured light depth sensors, each one has a brief description of the introduction of depth perception to the functioning performance of the device. Finally, it is performed a comparison between the different described sensors, in order to evaluate and explain the selected sensor attended in chapter 5.

### 2.2.1 Stereo Camera

Stereo camera is a type of camera which uses separate image sensors in each lens to simulate human stereoscopy (that's where the name "stereo" comes from). Using this type of camera, the

user has the capability to capture images that are instantly rendered in 3D. To do that, the camera has to process three distinct elements, such as the foreground, the background and zero parallax. The foreground and the background are the elements that appear closest and farthest to the image, respectively. The zero parallax is defined as the zone beyond the elements mentioned before, and is also called default zone. With the purpose of sharing a depth view, the camera needs to compute the rendering of the images, calculating the disparity between the three elements [20].

The stereo camera is good to work outside since it's simple to handle and it has commodity hardware. The camera is used in photography and cinema industries. Besides, the depth perception that the camera is capable of can lead to some artifacts: for example, estimating depth for uniform color surfaces. Concluding, the camera has potential to develop a reliable job in some areas but, since it only manages to do low resolution depth perception, it is not the ideal choice for the project.

### 2.2.2 Time of Flight

The technology behind the time of flight (ToF) camera is changing the industry since it uses an active pixel sensor array together with an active modulated light source. These two elements enable the camera to illuminate the environment with the light source and then measure the reflection. Therefore, the difference between the amplitude and period of the illumination and reflection waves is calculated. The camera then converts the difference into a distance or depth. Using the distance between every pixel, the camera constructs a 2D array or depth map and uses each created voxel to render and create a point cloud (3D space). The cloud points can be grouped to generate a final mesh [21].

According to Marvin Lindner *et al.* [22], the camera is susceptible to a range of errors, such as noise, derived from the interaction between the point clouds, and therefore from the mesh. Another crucial error is the systematic wiggling error, which is originated from the deficient sinusoidal signal shape that is not the ideal for the analysis of the illumination and reflection differences, due to hardware and cost limitations.

Finally, ToF cameras represent a reliable use for the project, since they show a good resolution for depth analysis. However, the camera has some error problems that can harm the project's goal.

### 2.2.3 Structured Light Depth Sensor

The last sensor presented is the structured light (SL) sensor. Among the others, the principal target of this sensor is to acquire 3D information of the world. Usually, the sensor is constituted by a charge-coupled device (CCD) camera and a laser projector that emits a known pattern of features. The design allows the system to have reduced dimensions when compared to the normal stereo cameras.

Otherwise stated in the ToF camera, the structured light sensor uses a structured light pattern, generated when a laser beam spreads into a sheet-of-light (adapted from the standard light-sheet

fluorescence microscopy technique [23]). The contact of the beam into an object creates distortions which can be transformed in height differences.

Structured light is being used in different applications, such as robotic guidance [24], printed circuit board inspection [25], edge detection, depth measurement, etc.

When compared to the other two cameras presented, this sensor is the one that produces the most reliable depth, with good compactness, portability and accuracy [26]. This type of sensor can also transmit some errors in resolution, related to the fact that it only calculates the depth at discrete points and it has to interpolate between them, leading to a reduction of accuracy by the system.

## **2.3 Summary**

In order to choose the best sensor for the project, a comparison between the 3 types was conducted.

Table 2.1: 3 Types Comparison

|                       | Stereo Camera | Structured Light | Time of Flight |
|-----------------------|---------------|------------------|----------------|
| Depth Accuracy        | Low           | High             | Medium         |
| Low Light Performance | Weak          | Good             | Good           |
| Range                 | Limited       | Scalable         | Scalable       |
| Power Consumption     | Low           | Medium           | Scalable       |

By analysing table 2.1, in terms of resolution, the stereo camera has a lack of definition. On the opposite side, ToF and SL sensors describe a reliable depth resolution, with a slight advantage to the SL one. The SL sensor has a better accuracy and performance, regarding the errors and problems that come from the rendering and process of the images.

In conclusion, it is clear the best sensor to apply and use in the project is the structured light sensor. In chapter 5, the sensor's specific functionalities are described.

# Chapter 3

## Virtual Reality & Augmented Reality

This chapter will describe the importance of the use of AR, and for that reason, the history beyond the AR is presented in section 3.2. Since AR was born from VR foundations, the chapter begins with a summary related to the most iconic stages that helped the AR's industry to achieve a dominant position in the respective community. Therefore, the section 3.1 is dedicated to relate the VR history, since it helps to understand what are the lacking points in this technology and, consequently, the major advantages of the use of the AR technology.

To conclude this chapter, it is of major importance to introduce what is the role of AR in the project and how it will be crucial for the project's development. Note that, the AR system is already being used by the investigation group, owing to the fact that it shows advantages when compared to the standard VR system.

### 3.1 Virtual Reality

The concept of virtual reality is being used in many industries since creates a whole new perspective of the virtual environment. This kind of environment can be programmed to work in many areas of study, from the phones that are used in daily life, to the projects developed by the biggest companies in the world.

#### 3.1.1 Virtual Reality Definition

According to Matjaž Mihelj *et al.* [27], VR technology is defined as a composition of an interactive computer simulation, with the capability to create in the user the sense of living the virtual reality environment in real life. In order to create such simulation, the technology recognizes the user's senses and changes the sensory feedback information.

The humans depend on the information originated from the five basic senses. The way how the human acts, when facing a new activity, is the assembly of the information that comes from the sight, hearing, smell, taste, and touch. This way, the VR can create virtual senses, that can

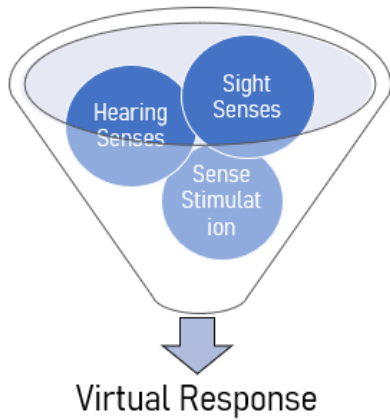


Figure 3.1: Brain Sensory Stimulation's.

originate real simulations to the human senses, particularly, the sight and hearing (figure 3.1). The human brain processes the real stimulation, but instead of answering to real activities, it answers to a problem created by a virtual system. In general, this is the way how virtual reality manages to create and induce a response by the user.

Another approach to the VR definition, was designed by Grigore C. Burdea and Philippe Coiffet in the book entitled *Virtual Reality Technology* [28]. The two authors include the VR technology as a product of boundaries between three I's, called the *Virtual Reality Triangle*:

- The first two I's define virtual reality as immersive and interactive. These features hold an interesting view. Since the immersion, with the help of a good interactive method, enables the experience where the user is surrounded by the created environment, making him feel like he is inside it and a part of it.
- The third and final vertex of the triangle constitutes the imagination feature.

As described before, the virtual reality environments are created by developers in order to answer some need or problem. On that account, the technology has numerous applications, being an important method to solve problems in areas, such as engineering, medical, military, etc [28]. For that reason, the imagination is an essential piece for the technology to work, and together with immersion and interaction, makes the VR technology an interesting and important instrument, to have in consideration not only in the present but in the future as well.

### 3.1.2 The History of Virtual Reality

The idea of VR was registered a long time ago, as the product of the human desire of not knowing what to expect from the imagination. The idea inspired Aldous Huxley, in 1931, to implement in the book *Brave New World* the proposition of *feelies*: movies that include sight and sound, integrating the sense of touch [29].

In 1935, the first description of the word *virtual reality* was described by the American science fiction writer Stanley G. Weinbaum, in the book *Pygmalion's spectacles*. In the book, an inventor creates a form of googles, that when used the user is fully immersed in an environment created by the inventor. There's a citation from the book where this idea is presented: "You are in the story, you speak to the shadows and they reply, and instead of being on a screen, the story is all about you, and you are in it" [30].

Later, in 1962, the first VR invention, called *Sensorama Simulator*, was constructed and patented by the inventor Morton Heilig [31], inspired by the knowledge described in Stanley Weinbaum's book. The mechanical device simulated a motorcycle ride through the city of New York, where the user was able to experience fan-generated wind and simulated noise and smell of the city [28].

The invention opened the doors to a whole new history chapter, such as in 1970, the American computer researcher Myron Krueger created the first environment, where the device could react to the human actions, using pressure sensors and video cameras. This way the described system was able to respond to the different user stimulations in order to move objects in the virtual environment. Therefore, the device presented itself as a major evolution to the system constructed by Morton Heilig, which was not implemented to recognize the user actions.

The emerging discoveries in the field were constantly updated year per year, due to the vast branch of applications, leading to the invention of the Cave Automatic Virtual Environment (CAVE) by Carolina Cruz-Neira, Daniel Sandin, and Thomas DeFanti at the University of Illinois, Chicago Electronic Visualization Laboratory, in 1992 (figure 3.2). The CAVE is a projection-based VR display, that uses real-time head tracking, interactive control, and binocular display. The user needs to stand in a room with screening walls displaying a virtual environment. The system was complemented by special glasses that give the user the perception of depth, regarding the fact that it was a primitive approach. Besides that, the CAVE was used by a high number of universities, but since it has a high price the system is not affordable for home version possibilities [27].



Figure 3.2: The CAVE at Electronic Visualization Laboratory, University of Illinois at Chicago [32].



Figure 3.3: Driving Simulator [34].



Figure 3.4: Cockpit of a flight simulator [35].

### 3.1.3 Virtual Reality Applications

As seen before, the large investments in this specific technology gave rise to a diversity of systems with countless applications in distinct areas of interest. This section will describe the sectors, where the VR changed the way how the industry faces the barriers from today. As said in the last section, the VR technology simulates and acquires the information originated from the user sensory stimulations, in order to build systems. Regarding that, some applications were constructed.

- **Flight & Driving Simulators:**

The application of VR for the purpose of creating flight (figure 3.4) and driving (figure 3.3) simulators, had a huge impact, for example, in the military field. Virtual flight environments help to prevent equipment damage, and more important is safer when compared to the real training habits, done by the military and commercial airlines flight trainees. Therefore, with VR simulators the companies can afford more quantities of trainees, ensuring the quality and safety of the training.

Nowadays, the simulators can be constituted by real cockpits, with floor-mounted chairs, and all the equipment that can be found in real airplane cockpits. The VR simulators can be developed to apply force feedback, with 3D real interaction with the user. The images can be generated along with the test simulation flight, promoting an authentic user immersion (3.1.1). Another advantage of the VR flight simulation is the possibility to model virtual worlds. In other words, the virtual environment can be programmed to simulate different climatic situations [33].

Besides the positives ideas about the simulators, it is important to know that no simulator has the ability to substitute the real action of flying an airplane or driving a car.

- **Motor Rehabilitation:**

When the nervous system is damaged due to some kind of accident, the rehabilitation of the patient is a slow and difficult process. Besides, in the majority of the cases, the therapy has high costs and do not assure the total motor recovery. VR has been suggested to solve these problems since can provide a unique path to acquire effective rehabilitation interventions.

Using the technology the patient's therapy is fruitful and personal, promoting better suitable exercises for each user. Thereby, the major rehabilitation goals, which are the improvement of self-confidence and quality of independent living, are productively and interestingly accomplished [36].

The VR technology is having a exponential use by a large number of therapeutics, becoming a great method to have in mind to help the patients recovery. Such approach, can be managed with the use of simple virtual environments or others more complex.

According to Witmer and Singer [37], when developing health therapy applications based on VR and VE some aspects need to be fulfilled. The two authors studied the psychology patterns beyond the normal therapy. For that reason, besides the immersion state (mentioned in 3.1.1) two other aspects were presented in the article. The involvement defines a psychological state originated from the user interaction with the VE stimuli. This state can be modified by the focus of the user in the activity/therapy, that can be justified on the degree of meaning that the person transfer to the stimuli. Although, the involvement depends on the equipment that's being used, since the focus decreases if, for example, the user is uncomfortable with the VE head-mounted display (HMD). The assembly of immersion and involvement, generate the presence of the user in all the process.

In conclusion, in order to increase the efficiency of the use of VR and VE in the motion rehabilitation therapies, is crucial to understand the psychological behaviour of the patient. Hence the presence of the user in the system will be much more accurate.

- **Telepresence & Teleoperation:**

The telepresence and teleoperation are applications that use the haptic feedback system - the haptic word represents the partnership between the force (simulating object hardness, weight, and inertia) and tactile (simulating surface contact geometry, smoothness, slippage, and temperature) feedbacks. The system is constituted by a tactile feedback technology that takes advantage of the sense of touch by applying forces, vibrations, or motions to the user. Hence, the haptic system allows the user to acquire information about an object by the sense of touch. Therefore, this type of tactile feedback is vital when applied to telepresence [38].

Hereupon, the telepresence defines the use of VR to allocate the user in a constructed virtual space allowing him to interact through forces and touch the VE objects.

On the other hand, the teleoperation was created to allow the user to interact with an object located in a distant place. The technology helps the science with the exploration and exploitation of spaces, that are unapproachable for the direct man access [39]. Hence, nowadays teleoperation is being used by NASA in mobile robots for the exploration of environments, such as the Moon, and Mars.

Besides the aerospace applications, the teleoperation is becoming an essential assisting device for the medicine, leading to the emergence of the telesurgery. Robot-assisted surgery is enhancing the ability and success of the surgeries [40].

Table 3.1: Teleoperation Applications

| Application                        | Description  | Industry                            |
|------------------------------------|--|-------------------------------------|
| GROPE IIIb Project                 | Haptic interaction with electrostatic molecule-substrate force simulations | Molecular Modelling                 |
| Early Bilateral Manipulators(MSMs) | Allow safe remote handling of irradiated material                          | Nuclear Engineering                 |
| Flight Telerobotic Servicer (FTS)  | NASA's robotic system operating in the space station                       | Aerospace Engineering               |
| Telesurgery                        | Remote surgery using a robot surgical system controlled by the surgeon     | Medicine                            |
| Unmanned Aerial Vehicles (UAVs)    | Aircraft without a human pilot on board and a type of unmanned vehicle     | Military, Surveillance, Agriculture |
| Remotely operated vehicles (ROVs)  | Used in deepwater to make hydrocarbon extraction                           | Extraction Companies                |

In table 3.1, are presented other applications, with a simple description, of the teleoperation in distinct industry sectors. Since are presented different inventions for different industry domains, with a special interest in the telesurgery (explained above). The table allows to see how global can be the use of this type of technology, and how important is the knowledge behind it.

- **Augmented Reality**

The augmented reality (AR) represents a VR application since it was originated from the knowledge acquired by the VR evolution. However, the technology constitutes an upgrade to VR because the simulation processes the real user environment, instead of using the VE described by the VR.

The AR technology will be portrayed in the next section (3.2), with a simple explanation about AR's history, current developments and status of the technology.

## 3.2 Augmented Reality: a new way to see the world

*“An augmented reality presents a virtual world that enriches, rather than replaces, the real world, instead of blocking out the real world.” [41]*

According to this sentence, AR is defined as a way to enrich the real world, then it is possible using this technology to see and create an environment beyond what our eyes see and feel, without leaving the real world. With the sense of the virtual world mixed with the real-world environment, the AR allows to understand and observe an object created in a VE incorporated in a RE. This aspect opens the insertion of AR in a large range of domains.

In the AR environment, user immersion acquires a new predominance. Instead of diving the user into a total VE, the AR type of user immersion allows different proportions between the VE and RE, achieving a level of immersion that can not be surpassed by any virtual equipment [42].

In order to understand the limits between the VE and RE, the different stages of the reality-virtuality continuum were explained by Milgram et al 1994 [4]. In figure 3.5, the two environments (VE and RE) are represented in each opposite end of the continuum. The left side consists in the environment constituted only by real objects and real scenes (real reality). As one moves to the right, the virtual side of the continuum begins to occupy some space in the system until the AR is reached. In this step, the optical see-through gains prominence, characterized by the visualization of the world surrounding the observer. Although, AR needs to maintain balance in the connection between the real world and the virtual objects. To accomplish that, the relationship between the reference frames of the real world, the user and the used camera, forces a rigorous knowledge.

Therefore, advancing to the right, the immersive component (which is a essential part of the VR technology, as mentioned in section 3.1.1) of the system grows, reaching the right side of the continuum, illustrated by the VE and VR. Note that, the mixed reality includes all the stages except the opposite ends.

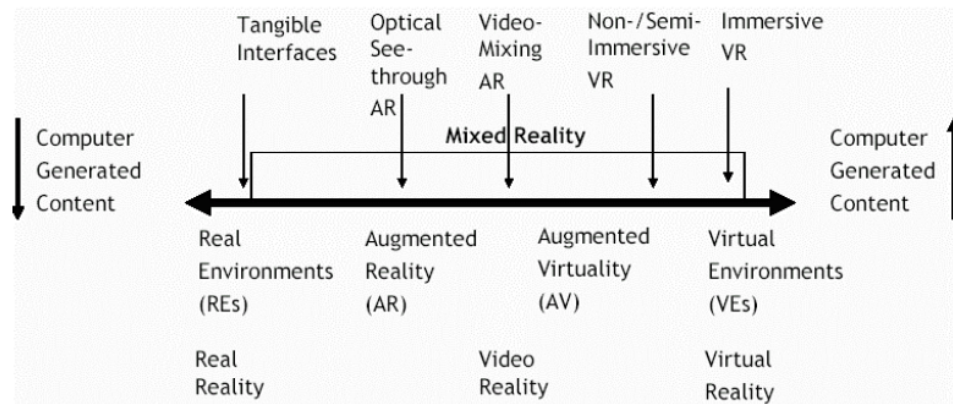


Figure 3.5: Reality-virtuality Continuum [42] [4].

### 3.2.1 The History of Augmented Reality

According to Oliver Bimber and Ramesh Raskar [43], the majority of the scientific community consider that the first impressions of the technology were made by Ivan Sutherland in 1965 [44]. In his work, the author implements for the first time the idea of a head-mounted three dimensional display (mentioned in 3.1.3), this invention was considered the birth of AR. Therefore, the three-dimensional display was acquired by showing to the user a perspective image changing as the user moves. Hence, Sutherland used mechanical and ultrasonic head position sensors to measure the position of the user's head, managing to calibrate the head position changes.

In 1992, Tom Caudell and David Mizell [45], introduce for the first time the term *Augmented Reality* since the technology was created to *augment* the visual field of the user with essential information in order to perform a task. The equipment used by the authors was a heads-up (see-thru) display headset (HUDset), tracking the movements of the user's head allowing them to have six degrees of freedom (6DOF), resulting in compensation of the variation in the user location and view orientation. In the work, the HDU technology was build as a proof of concept, by applying the AR to the manufacturing field.

Steven Feiner et al, developed in 1997, the Touring Machine, that is an experimental mobile augmented reality system (MARS), allowing outdoor and indoor user access to information that is spatially integrated to the real user surroundings [46]. The device was divided in three main parts:

- In outdoor, the user was equipped with the prototype backpack computer system connected to the head-worn display. Hence, using a tracking system with real-time-kinematic global positioning system (GPS), the user was capable to see the world augmented (figure 3.6).
- Hand-Held Display showing the map-based user interface.
- Indoor desktop allows the user to insert virtual information (such as messages or annotations) in the AR system, which could be seen in the outdoor activity.



Figure 3.6: User wearing the MARS prototype [46].

The continuous investment in the development of the technology gave rise to the work done by Hirokazu Kato and Mark Billinghurst [47]. Through the use of a precise virtual image, registration originated from computer vision techniques and HMD calibration the group managed to create an AR conferencing system. In the system, the users are the members of the conference or meeting and are represented on virtual monitors positioned in each user space. Therefore, the technology would allow the interaction between users remotely. This work marked the beginning of a project called SharedSpace developed by HITlab, that afterward culminated in two related technologies, the ARToolKit and the Magic Book.

### 3.2.2 Augmented Reality Application

Over the years, with the developments in image processing, computer graphics and monitor displays, the community was able to star sing the AR technology to improve many industry domains. With that in mind, some AR applications around the world are presented [48]:

- **Medical:** The applications of AR to the medical field are unlimited since imaging technology is an essential part of medical life. One example of the possible use of technology is image-guided surgery. With the use of AR, the doctor would be able to see the path to work with (CT scans and MRI data of the patient) before the surgery, and in real-time during the surgery. In this case, the AR stands for assisting technology to help the surgeon to make effective decisions [49].

Another possible application of AR was purposed by State, Chen et al. in 1994. Using the HMD an ultrasound technician could see a volume rendered fetus of a pregnant woman overlaid on her abdomen (figure 3.7c) [50].

- **Entertainment:** Nowadays examples of AR applied to entertainment activities and news businesses are frequently found. The majority of channel news use the AR to explain the weather reports, to do so, the real image is enhanced in digitally generated maps through a technology called chroma-keying.

The film business represents an AR growing industry, where the main reason is the development of more sophisticated and efficient special effects.

Also, the AR's special effects are being used to make, for example, the football games more easy to understand with the insertion, in recent years, of the offside line. In the USA the majority of the channels that broadcast baseball games use the technology to insert advertisements into specific areas of the broadcast image, using the augmented reality system provided by the Princeton Electronic Billboard [51].

- **Military:** The plane pilots are starting to use flight helmets with an information display. With the use of helmet-mounted visor displays the images of the users participating in the exercise could be shared.

- **Engineering Design:** Several complex engineering projects include exhaustive conversations between the project clients and designers. With a technology as AR the virtual meetings would allow to make the process more efficient. The AR would be able to display the project prototype in 3D, to the clients to see and discuss the different aspects. This idea was initially proposed by Hirokazu Kato and Mark Billinghurst [47], as described in the section 3.2.1 (figure 3.7b).
- **Robotics:** As applied by the VR, the robotics and telerobotics can be controlled also with AR. For example, an operator managing a robot to do some activity, with HMD equipped could see the results of attempting a particular motion with the virtual robot. Hence, the operator could decide to proceed or not with the motion after seeing the results [52]. Note that, this examples are not yet implemented.
- **Manufacturing:** In order to facilitate the work of many operators and technicians, the AR could apply a major evolution in the way how industries work. Using AR, when an operator looks to a new piece, the software could display the entire information about the specifications, highlighting possible modifications or errors to the manufacturing process of the piece.

In 2011, Francesca De Crescenzo et al applied AR for aircraft maintenance training and operations support [53]. The work was based on 4 key requirements for efficiency such as the fact that is user-centered, the implementation of a markless camera pose estimation, the efficiency of the authoring procedure, allowing simple and easy user interaction (figure 3.7a) [54]. In 2013, Google started selling Google Glass, which was a type of smart glasses, and the users could communicate with each other via the internet with natural language voice commands. Later in 2017, Google announced the Google Glass Enterprise Edition.

- **Consumer Design:** Virtual systems based in AR are already being used by some consumer design shops. For example, there are already in the market sensors that can do scanning 3D of a room, and using AR the client would be able to see if a specific house object is a good choice or not, regarding the implementation of the virtual object in the scanned room.



Figure 3.7: a) Head-mounted display prototype [53]; b) Remote user representation in the AR interface [47]; c) View of volume rendered fetus within pregnant subject [50].

### 3.2.3 Augmented Reality of Today

Normally, a AR system is constituted by a camera which captures the real-world environment surrounding the user and a graphics system with the job to implement the virtual objects. These virtual objects will be merged into the video of the real scene captured by the camera, originating the augmented video, that will be presented in a monitor.

With the constant developments of the technology, a new state of immersion was acquired with the implementation of the HMD and HUD (figure 3.8). Using the HMD see-through equipment the system needs to suffer some changes. The camera and the monitor will be implemented in the HMD, where the graphics system needs to be aware of the user's head position to create virtual objects. The monitor will finally display the augmented merged video across the HMD to the user's view [48].

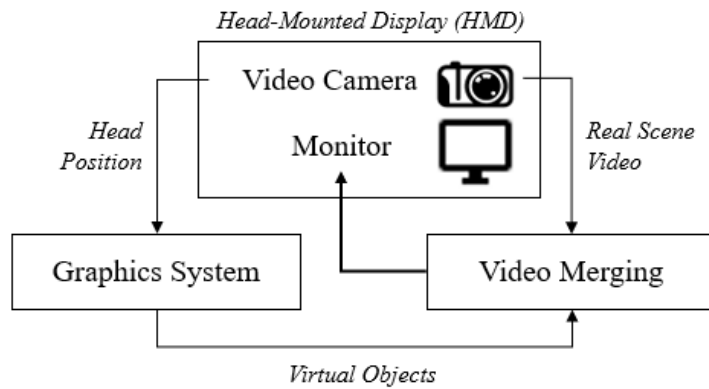


Figure 3.8: Scheme of the AR basic system.

The last approach has some advantages and disadvantages. It is a simple and efficient method to have an environment with information shared between the real world and the world created by the developer. However, it is clear that it is not possible to have interaction between the user and the virtual objects. Hence, the method lacks user possibilities throughout the whole immersion experimentation. For that reason, the system needs to find a way to track motions and positions of the user in the VE, in order to apply the acquired knowledge to the AR environment. Therefore, with a methodical strategy, it is possible to calculate the objects positions in the space. Hence, using motions positions as references, regarding the objects known positions in space, the user is capable to interact with the virtual objects. The method can be applied to an unlimited number of domains and industries, consequently, is of major importance the acquisition of the tracking knowledge, mentioned before.

### 3.2.4 UltraLeap: Leap Motion Sensor

Nowadays, the AR technology depends on a stable hand tracking system in order to manage the user to interact with the virtual objects. Some companies developed devices to do the recognition of the user's hands, such as the Leap Motion (figure 3.9) [55]. UltraLeap presented the Leap Motion Controller described as an optical hand tracking module. Through the capacity to discern 27 different hand elements, such as joints and bones, using light-emitting diode (LED) propagation and wide-angle lenses, the device can calculate the movements of the hands by recognizing the positions of each hand element. Regarding the recognition of the elements the controller does not create a depth map of the environment, however, it applies advanced algorithms to the raw sensor data.



Figure 3.9: Leap Motion device.

As stated above, the Leap Motion does not acquire data about the depth perception of the surrounded environment; consequently, the system needs to obtain this information from other source. This idea is explored in section 5.2, with the implementation of the structured light sensor.

### 3.2.5 Project NorthStar

As mentioned in 3.2.3, the UltraLeap company had a predominant role in the introduction of AR's technology into society. With the Leap Motion controller in the market, the company initiated the development of an open-source program called "Project North Star".

*"We envision a future where the physical and virtual worlds blend together into a single magical experience. At the heart of this experience is hand tracking, which unlocks interactions uniquely suited to virtual and augmented reality."* [56]

Hence using the Leap Motion Controller for hand tracking, a new way to create and explore augmented reality was introduced. Note that, the gold mine of the project is due to the fact of its open-source method. Even with all the positive points about this technology, the NorthStar (NS) solution not represents a complete AR solution. Therefore, developers could share information

and knowledge, and this allocation of ideas led to the creation of the first NS headset. On that account, the constant information contribution between the different developers is leading to a future where the physical and virtual worlds blend into a single experience.

### 3.2.5.1 NS headset

The NS headset is composed of different pieces which complete a two modular assembly:

- Mechanical: The components that represent this part of the headset are the optics bracket, the headgear with hinges, and the halo (where the electronics are located). In figure 3.10 the components of each one of the mechanical parts are showed. Besides that, in table 3.2 the number of components that need to be assembled to complete the headset is referenced.
- Electrical: In order to achieve the electronics of the headset, a proper software builds the AR Display Board firmware.

With the characteristic of being an open-source project, it is of major importance that anyone can put together the distinct parts of the headset. For that purpose, UltraLeap made available a mechanical guide with all the instructions to develop the headset.

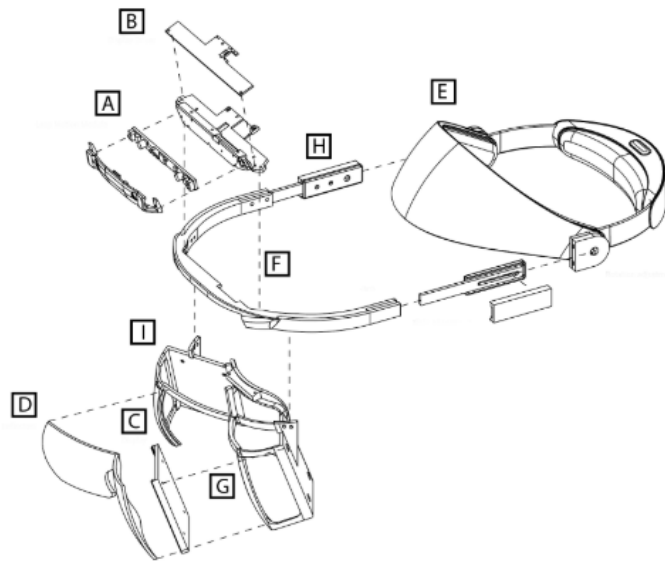


Figure 3.10: Headset Parts.

Table 3.2: Figure 3.10 Label

| Ref. | Part Name                       | Quantity       |
|------|---------------------------------|----------------|
| A    | Leap Motion Controller          | 1              |
| B    | Display Driver                  | 1              |
| C    | 3.5-inch 120Hz LCDs             | 2              |
| D    | Acrylic reflectors              | 2              |
| E    | Headgear                        | 1              |
| F    | Self-tapping screws for plastic | -              |
| G    | Machine screws M2.5 x 6mm       | -              |
| H    | Hinge fasteners, #10-32         | -              |
| I    | Al. bar stock 10x3mm            | 12-in [300 mm] |
| J    | 3D printed parts                | -              |

It is important to note that the components responsible for the image output are the liquid-crystal displays (LCDs) and the poly(methyl methacrylate) (PMMA) reflectors represented in the figure 3.10 by the C and D letters, respectively.

The reflector's ellipsoid form allows that the light emitted from one focus reflects off its surface and focuses it on the second focus, with its perimeter being chosen empirically by minimizing the system distortion. Hence, it was concluded that the best dimensions for the reflectors are around 75x75mm with a thickness equal to 2.5mm. Finally, the outside surface of the reflectors requires an anti-reflective coating to inhibit a secondary light reflection and consequently image degradation.

Having introduced the NS project and the headset, it is important to say that the work will use it as the main foundation for the AR development.

# Chapter 4

## Alzheimer's Disease

This chapter will be dedicated to the introduction of Alzheimer's Disease (AD). The procedure to apply to this neurodegenerative disease to the context of the work is explored in the present chapter.

### 4.1 Neurodegenerative Disease

Neurodegenerative diseases are commonly diagnosed as cases of dementia, which becomes worse with time. According to the Alzheimer's Association [9], it is estimated that in the United States 5.8 million people have lived with AD in 2019. As stated by H. Niu *et al.* [57], in 2050 the number of European individuals affected by dementia will reach 106.8 million, including an upward incidence trend of 87% in Europe for the 2010-2050 period [58].

Dementia is a clinical syndrome that can be caused by the neurodegeneration of specific tissues such as brain cell systems in the case of AD. Since the brain is responsible for the majority of human body activities, it is clear that an impairment of the organ can cause deterioration in cognitive function, and body behavior. Therefore, it is important to study and invest time and resources investigating AD, which corresponds to 50-70% cases of dementia worldwide [59].

Over the years, AD has been a theme of discussion for many researchers as treatments only delay the evolution of the disease. According to Clifford R. Jack *et al.* [6] there is evidence that supports abnormal processing of  $\beta$ -amyloid peptide, leading to the formation of A $\beta$  plaques in the brain, which is then the precursor to the neurodegeneration.

Since the reasons for the formation of the A $\beta$  plaques are not known, and the incidence rate of the disease is increasing, it is important to understand which are the risk factors. As stated by the Alzheimer's Association in an article published in 2019 [9], the main risk factors are age, the presence of  $\epsilon 4$  form in the ApoE gene, and family history.

Since age is identified as the main risk factor, it is clear that it gains more preponderance as the world population grows older, and the average life expectancy increases. However, studies cannot confirm that AD dementia is a consequence of aging, give age alone is not a precursor of AD.

AD was initially documented as a sporadic disease, however recent studies claim that the disease can occur due to genetic factors, such as the existence of  $\epsilon 4$  allele in the apolipoprotein E (ApoE). According to G. Lucotte *et al.* [60], ApoE has a role in the lipid transport, metabolism, and targeting of the  $\beta$ -amyloid peptide in the brain, therefore alterations in this gene can lead to dissimilar A $\beta$  metabolism.

According to N. T. Lautenschlager *et al.* [61], elderly relatives of AD patients represent a crucial group for the study of the genetic factors that can lead to AD. The study points to men having a higher probability of developing hereditary dementia when compared with women. However, women are in the first instance more susceptible to AD, when not considering the hereditary aspect.

With this in mind, it is important to notice that the three risk factors can be developed individually or simultaneously, being the aging process the main factor of the increase of AD cases over the years.

## 4.2 Investigating AD

To study AD, there are distinct techniques and approaches; one of them is the thickness variation analysis between brain lobes. The majority of the research is being conducted using structural magnetic resonance imaging (MRI), which allows the study of structural brain anatomy. Thereupon, MRI scans enable to study the evolution of brain cortical thickness and lobe volume. For that purpose, AD clinical trials implement this imaging technique in order to create a data set to enable thickness analysis [62].

Li, Chuanming *et al.* [63] studied the differences in the brain cortical area between MCI and AD patients. The author found that the cortical area was altered when comparing the two diagnostics. Specifically for the AD patients, a significant decrease in the cortical thickness in the majority of the brain studied areas was found. The study also reported differences in the cortex atrophy pattern for the MCI and AD.

Regarding the same study concept. Lehmann, Manja *et al.* [64] made the comparison between the posterior cortical atrophy (PCA) patients and the cortical atrophy present in AD patients. The author found that when comparing healthy and AD patients, cortical thickness is thinner for the AD patients in the temporal lobe, with differences in the parietal lobe as well. Furthermore, the author observed that the left cortex is more affected than the right cortex.

### 4.2.1 ADNI Database

To aid the research and study of AD through the improvement of clinical trials, the Alzheimer's Disease Neuroimaging Initiative was established as a publicly available database with material essential for the disease study.

In general, ADNI is defined as a multisite longitudinal observational clinical/imaging/biomarker exploration, which aggregates data from different U.S. universities [65]. On top of that, ADNI provides distinct unique sets of medical imaging such as MRI, PET (positron emission tomography), including measures of cerebral spinal fluid and blood biomarkers.

Since it is known that the AD precursor consists of the accumulation of A $\beta$  amyloid in some areas of the brain and this phenomenon promotes neurodegeneration through synaptic dysfunction. ADNI available data allows the exploration of the differences and the visualization of detectable changes in A $\beta$  aggregation with CSF analysis.

Another example of the capabilities of ADNI is presented in figure 4.1, consisting of a nine MRI's set extracted from the ADNI database. The images were captured from a axial point of view using a 3-plane localizer (scan destined to find the subject's head). Besides the set of MRI's, the database allows the researcher to explore information about the diagnostic result, age, and genre for each patient. In the specific case of the patient in which the MRI's set is represented in figure 4.1, the patient is a 85 year old male, who was labeled as cognitively normal (CN).

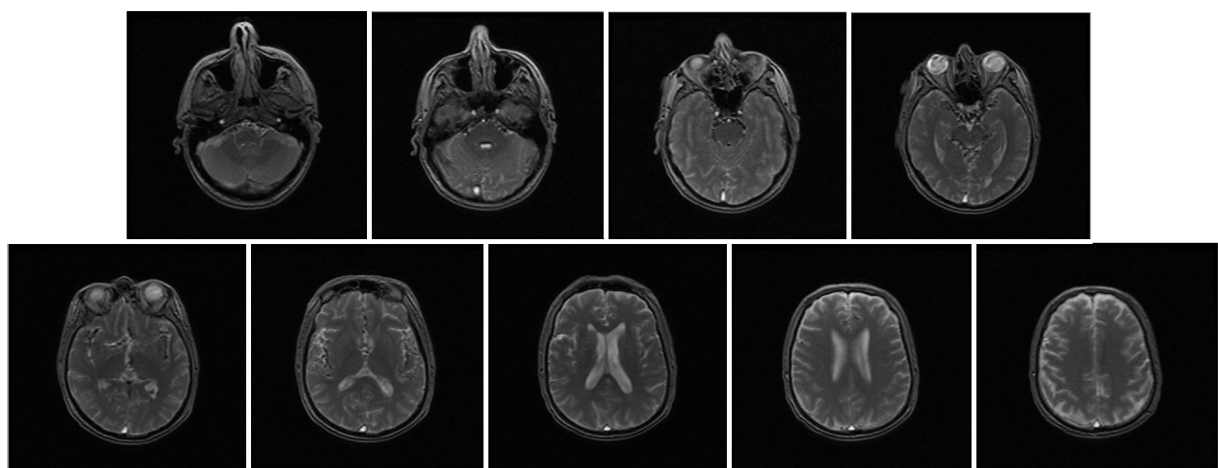


Figure 4.1: ADNI based patient MRI's.

ADNI uses a system for the labeling of patients (cohorts) in terms of cognitive brain activity. Since the creation of the database, 4 major studies were performed.

- ADNI 1: The study was based on three main cohorts: CN, MCI, and AD, in order to accomplish objectives such as the creation of an available data repository for testing of theories based on clinical and biomarker data, and help the analysis of longitudinal brain changes. For that purpose, the study had a participation pool of 200 normal control, 400 MCI, and 200 AD subjects.
- ADNI GO: For the second study, the MCI cohort was modified to create de EMCI (early mild cognitive impairment). The analysis of CSF and blood was done for the new group, with a special interest in the extraction of samples for ApoE genotyping. Into the study, 200 new EMCI subjects were enrolled.

- ADNI 2: As in the previous study, the LMCI cohort (late mild cognitive impairment) was implemented. With the inclusion of 150 CN, 150 EMCI, 150 LMCI, and 200 AD new subjects, the study was focused on the extraction of DNA and RNA through blood samples collection, and the validation of clinical diagnoses and imaging from the previous studies.
- ADNI 3: The study was performed to help the exploration of the biomarkers, measuring their differences, to forecast patient cognition decline using PET imaging. The study also focus on the discovery of other AD precursors such as proteins and genes. In order to accomplish the study objectives, 135-500 CN, 150-515 MCI, and 85-185 AD new subjects were enrolled.

It is important to notice that when labeling the subjects into different cohorts, each one requires a specific type of evaluation. The subjects are classified as CN when there are no signs of mild cognitive impairment, or dementia. For the SMC cohort, the subject report is quantified using the Cognitive Change Index [66][67] and the Clinical Dementia Rating of zero [68]. Finally, the MCI class requires the Wechsler Memory Scale Logical Memory II [69][70]. The previous method allows the distinction of the MCI cohort into EMCI and LMCI.

#### 4.2.2 Desikan-Killiany Brain Atlas

In order to fully understand data extracted from the ADNI database, there are automatic labeling systems to divide the human cerebral cortex into multiple lobes, such as the Desikan-Killiany brain atlas. The authors of the atlas explain that the system was established using gyral based regions of interest (ROIs). Therefore, 35 regions for each brain hemisphere were created (figure 4.2). In table 4.1 the distinct ROIs are listed corresponding to the previously mentioned figure. The different ROIs represented in table 4.1 can be organized according to the main 5 cortex lobes which are frontal, parietal, occipital, and temporal lobe. As stated by Rahul S. Desikan *et al.* [71], the author grouped the regions according to the following list:

- Frontal: Caudal Middle, Pars Opercularis, Parsorbitalis, Pars Triangularis, Paracentral, Rosstral Middle, Superior, Frontal Pole, Precentral, Lateral Orbital, Medial Orbital and Insula.
- Occipital: Lateral Occipital, Lingual, Pericalcarine and Cuneus.
- Parietal: Precuneus, Inferior and Superior Parietal, Supramarginal and Postcentral.
- Temporal: Inferior, Middle and Superior Temporal, Temporal Pole, Transverse Temporal, Entorhinal, Parahippocampal, Fusiform and Superior Bank.
- Cingulate: Isthmus, Rostral Anterior, Caudal Anterior and Posterior.

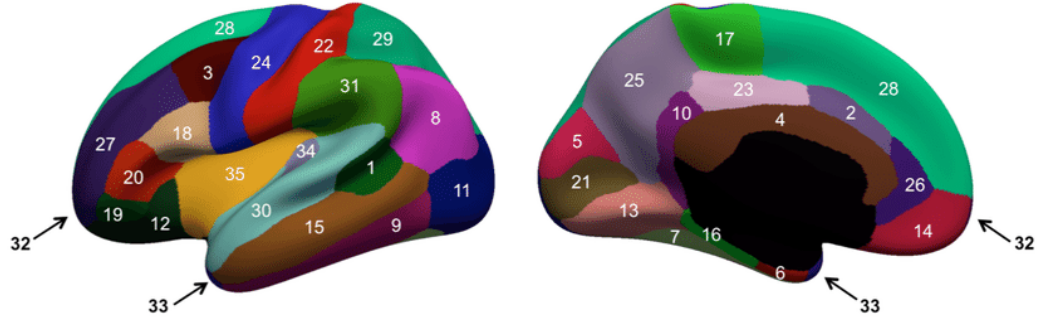


Figure 4.2: Desikan-Killiany Brain Atlas.

Table 4.1: Figure 4.2 Label

| Number | Region                         | Number | Region                            |
|--------|--------------------------------|--------|-----------------------------------|
| 1      | Bank of the Superior Temporal  | 19     | Pars Orbitalis                    |
| 2      | Caudal Anterior-Cingulate      | 20     | Pars Triangularis                 |
| 3      | Caudal Middle Frontal          | 21     | Pericalcarine Cortex              |
| 4      | Corpus Callosum                | 22     | Postcentral Cortex                |
| 5      | Cuneus Cortex                  | 23     | Posterior-Cingulate Cortex        |
| 6      | Entorhinal Cortex              | 24     | Precentral Gyrus                  |
| 7      | Fusiform Gyrus                 | 25     | Precuneus Cortex                  |
| 8      | Inferior Parietal Cortex       | 26     | Rostral Anterior Cingulate Cortex |
| 9      | Inferior Temporal Cortex       | 27     | Rostral Middle Frontal Gyrus      |
| 10     | Isthmus-Cingulate Cortex       | 28     | Superior Frontal Gyrus            |
| 11     | Lateral Occipital Cortex       | 29     | Superior Parietal Cortex          |
| 12     | Lateral Orbital Frontal Cortex | 30     | Superior Temporal Gyrus           |
| 13     | Lingual Gyrus                  | 31     | Supramarginal Gyrus               |
| 14     | Medial Orbital Frontal Cortex  | 32     | Frontal Pole                      |
| 15     | Middle Temporal Gyrus          | 33     | Temporal Pole                     |
| 16     | Parahippocampal Gyrus          | 34     | Transverse Temporal Cortex        |
| 17     | Paracentral Lobule             | 35     | Insula Cortex                     |
| 18     | Pars Opercularis               |        |                                   |

The two brain hemispheres are divided into four main lobes: frontal, occipital, parietal, temporal. Each one has a specific role in the harmonious functioning of the human system. Note that the two hemispheres are connected by the corpus callosum region.

The frontal lobe is associated with language, personality (affection and mood), and self-awareness [72]. The occipital lobe is related to visual processing. Sensory information (touch, temperature, pressure, and pain) is controlled by the parietal lobe. Finally, there is the temporal lobe that is responsible for auditory information. Since it contains the hippocampus, the temporal lobe has a major memory role, also monitoring the learning and emotional component [73].

### **4.3 Conclusion**

AD is a matter of study for many researchers, due to its incidence. Since there is no approved theory for the formation of the amyloid plaques, there is a lot of interest in the investigation of the process. For that purpose, the analysis of the cortical thickness is being studied, in an attempt to better understand what is happening concerning the cortical brain atrophy.

In section [4.2](#), two distinct studies related to cortical thickness were indicated. Therefore, the objective of the dissertation work is to develop an AR technology where the user can analyze and visualize the cortical thickness differences when comparing the distinct cohorts from the ADNI database. The main goal is to achieve the same results as the studies mentioned previously.

## Chapter 5

# Methods I: Hardware Implementation

For the dissertation work, several steps were defined as being the main components of the project. Firstly, in order to have a superior AR experience, the calibration of the sensors and headset lenses is required. The second step describes the implementation of the Structure Core sensor into the headset and consequently into the Unity project.

Note that, being the methods component of the work divided into three major components, each one has its specific role and is crucial for the AR system performance (figure 5.1).

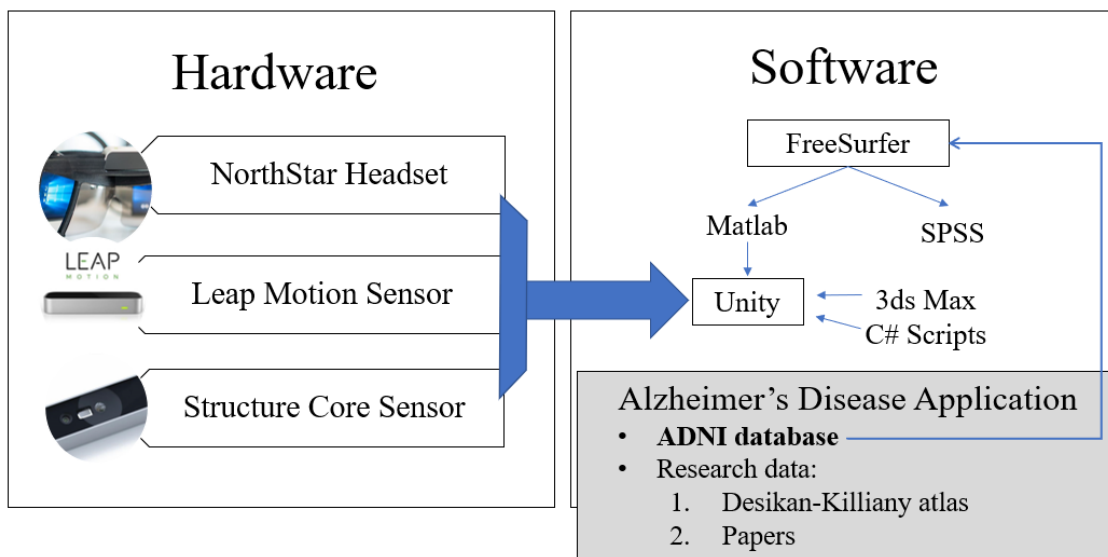


Figure 5.1: 3 main components of the work.

The work is based on the ADNI data processing by FreeSurfer software. Such data is then submitted to statistical analysis in SPSS and Matlab. In this last case, the results are sent to Unity. The whole system is controlled inside an AR environment which is in continuous interaction with the hardware components.

## 5.1 Calibration

The calibration process will be divided in 3 different stages. Note that the lenses calibration uses the Leap Motion controller. Therefore, it is of major importance a satisfactory sensor assessment before the lenses calibration.

### 5.1.1 Leap Motion

The lack of sensor alignment at the beginning can cause problems such as persistent jumpiness, tracking data discontinuities and poor tracking range.

With the purpose of achieving the best performance, Leap Motion's manufacturers developed a calibration system that can be accessed using the sensor control panel. An example of this type of calibration can be seen in figure 5.2a.

### 5.1.2 Headset lens

After the Leap Motion assessment, the sensor is used to calibrate the lens. Several ways to access the process were developed such as the creation of a toolbox using Unity software (figure 5.2b). Another way is the use of 4 stereo cameras to assist the positional tracking and optimization of the originated reflection image. The toolbox process has some advantages concerning the stereo camera aid process since uses a more practical and easier environment to work. Therefore, it originates a reliable calibration file in a short time. Afterward, the file is used in Unity's project environment to assist in the augmented reality performance.

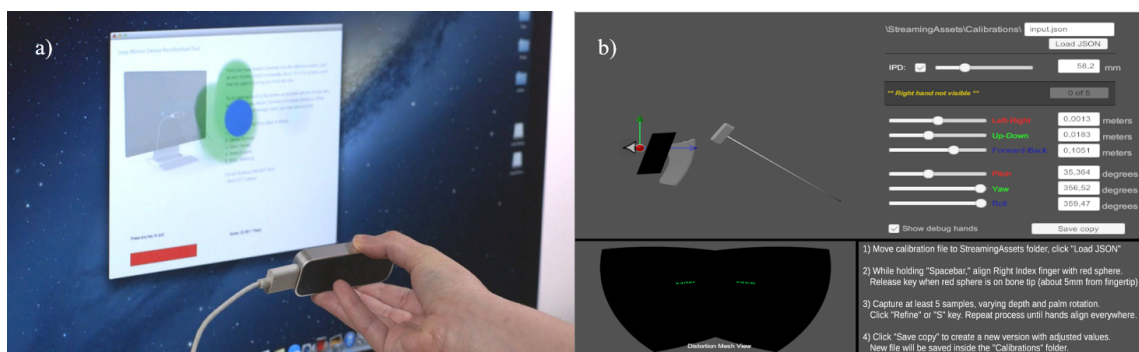


Figure 5.2: a) Leap Motion Controller Calibration; b) Lens Calibration Toolbox.

## 5.2 Structure Core

In this section, the SL sensor will be presented and implemented using Unity software. Since the depth values need to be acquired to facilitate and improve the immersion of the user, the sensor will be used in the dissertation work aggregated with the Leap Motion and the NS headset.

### 5.2.1 Sensor: Structure by Occipital

The sensor type selected to calculate the depth perception of the objects around the environment and all the systems is the SC sensor. Note that the reasons to choose this type of sensor are explained in chapter 2.2. Therefore, the chosen sensor was the Structure Core developed by company Structure by Occipital.

To understand the proposed application, the sensor specifications and structure need to be studied in detail.

### 5.2.2 Structure Core in detail

The SC sensor uses two essential components: a CCD camera and a laser projector. In the particular case of SC, the sensor has two infrared global shutter cameras, an ultra-wide vision camera and a laser dot projector. The efficiency of the sensor relies on the geometrical relation between the three cameras and the projector.

Structure by Occipital developed SC based on the Primesense system [74], with a depth resolution of 1280x960 and frame rate of 1280x800, a range of 0.3 to 5 meters depending on the scene and lighting conditions. Depth processing is done using NU3000 ASIC [75]. The Inuitive company created NU3000 ASIC with open software architecture, enabling the support of both proprietary and 3rd party software. The processor allows the implementation of complex computer vision functions, accurate 3D imaging, and 3D vision applications for consumer devices.

In Figure 5.3, the main hardware elements of the SC sensor are represented. Note that the processor (NU3000 ASIC) is connected to all the remaining elements, with special interest to the connection to the stereo IR camera, VGA camera and the IR pattern projector. The sensor uses a Bosch BMI055 IMU (inertial measurement unit) which is an electronic device that measures and reports a body's specific force, angular rate, and orientation through the use of an accelerometer - measures the acceleration of a body in its own instantaneous rest frame - and a gyroscope - measures the angular rate. The two IMU's elements have 6 degrees of freedom. [76]

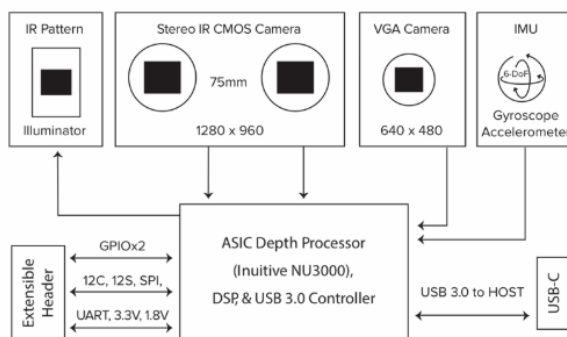


Figure 5.3: Structure Core Hardware Architecture [75].

The sensor can be acquired with monochrome or a color version. However, the color version has a smaller field of view. Consequently, since this parameter is essential for the depth measures, the group decided to purchase the monochrome version of the SC sensor.

### **5.2.3 Sensor Implementation**

To make the sensor implementation, two paths were considered. The company provides examples to allow the user management of the sensor. Therefore, using the examples, it was possible to activate the sensor console and, consequently, implement the sensor using the Unity project software. In figure 5.4, the NS headset with the SC (above) and Leap Motion sensors is represented.



Figure 5.4: Headset with SC and Leap Motion sensors.

# Chapter 6

## Methods II: AR & 3D Models

In the present chapter, the main foundations of the AR environment used for the dissertation work will be described.

As mentioned before, our version of the AR system is based on project NS. Hence, the creation of the AR environment is the first step, followed by the implementation of the SC sensor, reported in chapter 5.

Concluded the integration of the depth sensor and having established a stable and efficient connection with the AR environment, the introduction of 3D models is the next step.

### 6.1 AR Development

The AR system is based on the project NS, therefore it uses the Leap Motion controller in order to acquire hand tracking. Besides that, the system shares the interaction between the SC and the Leap Motion sensor. Hence the hand tracking component of the work is developed under a GO called ARCameraRig. The GO is already established and can be found in the NS project available LeapAR Unity package [77].

Regarding the use of the Leap Motion sensor, the goal is to get hand data (both static and/or dynamic) from the sensor into the Unity project. In order to achieve its purpose, the Leap Motion Unity package software is composed of different assets, plugins, and prefabs.

- The prefabs component is essential for the visualization of the virtual hands in the Unity scene and consequently in the AR immersion. In specific the use of the Leap Rig prefab.
- The core of the sensor has some elements that are called the providers. Firstly, the LeapProvider helps to define the interface to retrieve frame data. The LeapServiceProvider establishes the connection with the Leap service that provides frame objects to receive the hands Leap data. Another important provider is the LeapXRServiceProvider, that manages

to calculate the differences in the time tracking between the sensor and the HMD pose tracking. In other words, the provider has in account the different tracking latencies for the two devices (HMD and sensor), to enhance the global tracking system.

- The hand model manager is another important feature since it generates the transmission of data along with the hand models. The hand models are also used to represent the three-dimensional virtual hands called capsule hands. In figure 6.1 the scene view of what the NS package offers is shown, with a representation of the capsule hands.

The information concerning the Leap Motion sensor software specifications was extracted from the Leap Motion online page [78].

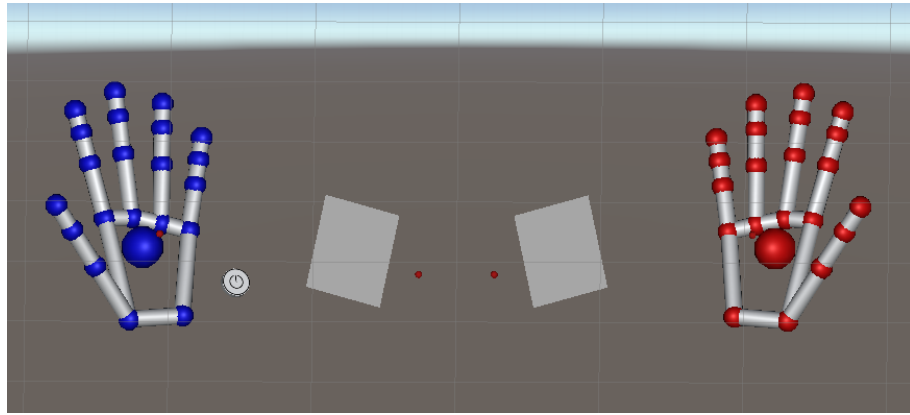


Figure 6.1: AR virtual hands representation in Unity.

For the purpose of the work the ARCameraRig has the same conceptual behaviour as the Leap Rig (LeapAR package). Hence, uses the same components mentioned in the previous list. Besides that, a two camera system was implemented. The use of two cameras, one for each eye, increases the user perspective immersion.

Regarding the predominant focus in the interaction between the user and the virtual objects, the system operates using the hand model manager and the interaction manager. Therefore, through the data received from the leap provider (as the hands are tracked), the hand model manager pipes the information to the hand models.

The interaction manager is constituted by the interaction engine, that allows the user to contact with virtual physical objects, using hand interactions such as, hover, touch or grasp.

In general these are the overall main roots for the AR interaction user system. These features are used in the 3D model manipulations (section 6.3), being the 3D models one of the virtual physical objects used in the AR work.

## 6.2 3D Models

The introduction of 3D models into the AR environment is a process with major relevance for the purpose of the work, in specific the insertion of a skull and brain models. In this section, the

models application will be explored, and also, the user manipulations in AR for the referenced models. Note that, the 3ds Max software was used to arrange the model meshes.

### 6.2.1 Models Application

Regarding the models application, the relevant aspects are the model sources, and the number of meshes that compose each model. Since neither the skull nor the brain 3D modeling were objectives of the work, these models were extracted from open model libraries.

#### 6.2.1.1 Skull

The skull model was obtained from the online page Sketchfab [79], and is constituted only by two meshes. The model is licensed by the Creative Commons organization [80].

Since the model is used exclusively for AR manipulations (section 6.3), there is no need for a better mesh split model. Hence in figure 6.2 is represented the skull 3D model.

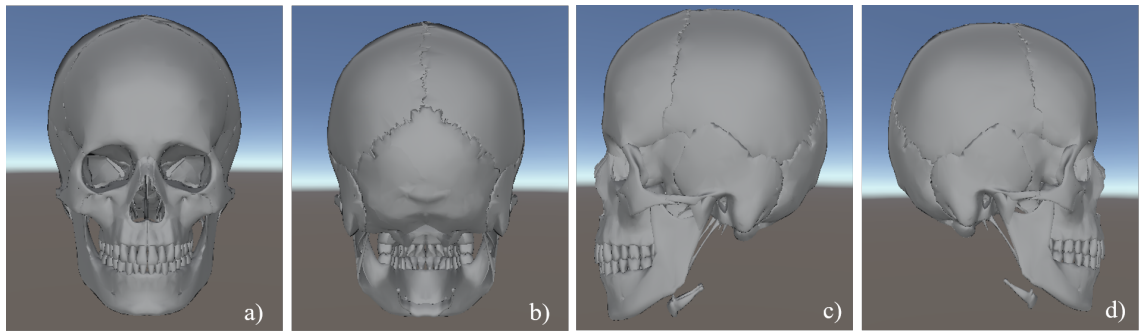


Figure 6.2: Skull model different views: a) Front b) Back c) Left side d) Right side.

#### 6.2.1.2 Brain

The brain 3D model was extracted from an available 3D human brain library created by Anderson Winkler, the model was constructed using magnetic resonance imaging [81]. The products available on the website are licensed by the Creative Commons organization [80].

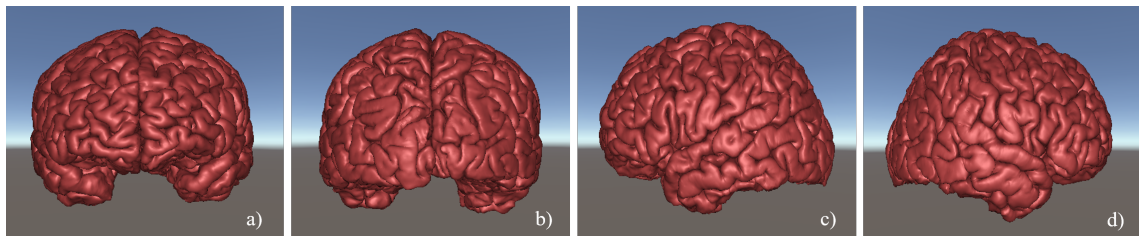


Figure 6.3: Brain model different views: a) Front b) Back c) Left side d) Right side.

In figure 6.3 is represented the selected brain model. The model is constituted by 66 meshes (33 for each hemisphere).

There is a reason for the selection of this specific type of model, since the brain modeling author, mentioned previously, model the cortical mesh split according to the Desikan-Killiany atlas. Therefore, the meshes are correspondent to the regions shown in table 4.1, however 2 regions are not represented which are the corpus callosum, and bank of the superior temporal.

### 6.3 3D Model Manipulation in AR

As mentioned in section 6.1, for the manipulation of the 3D models such as the brain and the skull, the system uses the interaction engine. Therefore, each model has two components, the box collider, and the rigid body properties. These components help to define the interaction behavior for each model. The box collider describes the hit box for the model. Since the virtual hands are responsible for the interaction, whenever the hand's interaction points hit the box collider, the model suffers physical behaviors. Besides that, the rigid body component attributes physical properties to the models, such as mass, and drag.

Hereupon, note that the main physical interaction between the models and the user virtual hands is the grasping reaction.

#### 6.3.1 Model Selection Menu

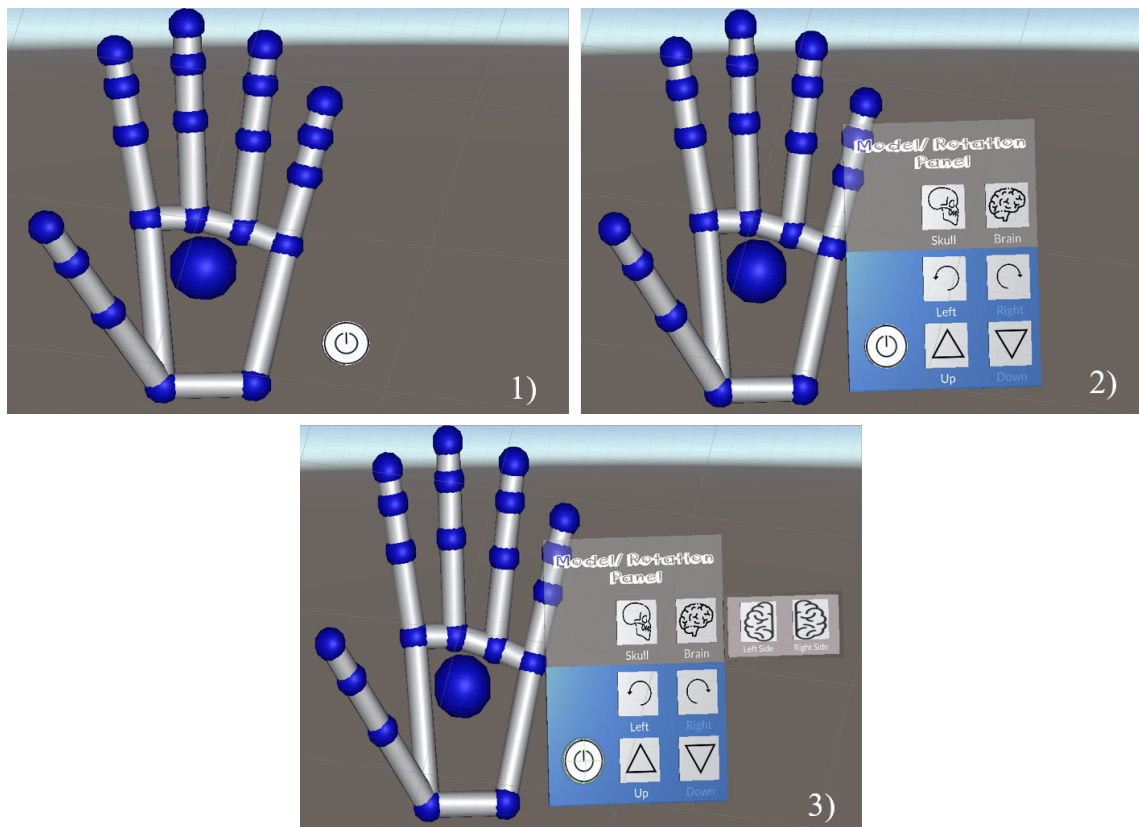


Figure 6.4: Representation of the model rotation/selection menu.

The menu seen in figure 6.4.2) allows the user to select the models. When a selection is made, the chosen model is activated and it appears in the user AR environment. Specifically, if the user presses the brain model button, another minor menu will appear, giving the user the capability to activate/deactivate each hemisphere (figure 6.4.3). Another function of the menu is to grant the capacity to rotate (right, left, up, and down) the model by allowing the user to press the buttons that can be found in the menu's blue rectangle.

The menu is controlled by an on/off button (figure 6.4.1). The button is attached to the left hand and, consequently, the menu is also attached to the same hand.



# **Chapter 7**

# **Methods III: AR for Alzheimer Disease Study**

In this chapter is documented the use of the AR system already presented in chapter 5 and 6 for the study of AD. For that purpose, the AR technology is integrated with Unity and Matlab.

The ADNI database (mentioned in section 4.2.1) is used to acquire cortical thickness data from patients with different cohort types (CN, SMC, MCI and AD). Therefore, the FreeSurfer software was used to analyze and process the ADNI human brain MRI's.

## **7.1 Proof of Concept**

As indicated in section 4.3, the goal is to develop a technology where the user can visualize and reproduce the relevant scientific results of the reference studies considered ([63][64]), with the particularity of being immersed in the AR environment.

To achieve the proposed objective two studies were conducted.

The first study is aimed at the analysis of the differences in the ROIs cortical thickness using statistical methods. Hence is possible to evaluate the occurrence of cortical atrophy when comparing the ADNI's cohorts. The main goal is to reproduce the scientific results of the studies in section 4.3.

The second study targets the ADNI data processing using Matlab, in order to establish a connection with the Unity software and consequently with the AR developed system. The objective is to visualize the scientific results and derive the relevant conclusions, presented in the first study, using the AR environment.

### **7.1.1 ADNI Cortical Thickness Data**

Data used in the preparation of this thesis were obtained from the ADNI database (adni.loni.usc.edu). The ADNI was launched in 2003 as a public-private partnership, led by Principal Investigator

Table 7.1: ADNI Subject Characteristics

|             | Cognitively<br>Normal | Significant<br>Memory Concern | Mild Cognitive<br>Impairment | Alzheimer's<br>Disease |
|-------------|-----------------------|-------------------------------|------------------------------|------------------------|
| Number      | 50                    | 28                            | 158                          | 106                    |
| Male/Female | 22/28                 | 8/20                          | 96/62                        | 57/49                  |
| Age         | 74.08 ± 6.28          | 72.97 ± 4.70                  | 73.01 ± 6.91                 | 74.55 ± 8.18           |

Michael W. Weiner, MD. The primary goal of ADNI has been to test whether serial MRI, positron emission tomography (PET), other biological markers, and clinical and neuropsychological assessment can be combined to measure the progression of MCI and early AD.

As said in section 4.2.1, ADNI is a publicly available MRI's database. Each set of patient MRI's can be processed in order to acquire study material such as cortical thickness for each brain ROIs.

The ADNI database includes data on 342 subjects. The subject's classification and main characteristics are shown in table 7.1. As expected, the cohort of AD subjects are older on average, due to the fact that aging is the main risk factor for the development of the disease.

### 7.1.1.1 FreeSurfer for Data Extraction

As mentioned before, FreeSurfer was the chosen software to make the extraction of cortical thickness data from the MRI's in the ADNI database [82]. FreeSurfer is an open-source software with the capability to process brain MRI images. Hence, FreeSurfer is being used by many AD investigation groups, with the procedure being validated and reported by Dale *et al.* [83] and Fischl *et al.* [84].

The image processing handled by FreeSurfer among others includes skull stripping (removal of the skull and non-brain tissue), intensity normalization, tessellation of the gray matter white matter boundary, automated topology correction [85], and surface deformation following intensity gradients to optimally place the gray/white and gray/cerebrospinal fluid borders at the location where the greatest shift in intensity defines the transition to the other tissue class [83]. Having performed the previous steps the parcellation and registration of the cortex data according to the Desikan-Killiany atlas was accomplished [71]. Therefore 35 cortical thickness measures were generated for each hemisphere [86]. However, only 33 measures will be included in the study, since the 3D brain model has only 33 meshes for each hemisphere (mentioned in section 6.3).

### 7.1.2 1<sup>st</sup> Study - ADNI Statistical Analysis

The number of subjects included in this study is presented in table 7.1. Note that, the subject data (cortical thickness, age, gender, and eTIV (estimated total intracranial volume)) was obtained from the processing using FreeSurfer. The study consists of the statistical analysis of the ROIs, in order to analyze the thickness evolution behavior of the SMC, MCI and AD cohorts when compared with the control group (CN).

### A. Data Processing

The data was analysed and processed using the SPSS software. Multivariate general linear model (GLM) with age, gender, and eTIV as covariates was performed. Therefore the average thickness values for the distinct ROIs were obtained. The comparison between the SMC, MCI, and AD cohorts with the CN group was obtained, using the resulted average results.

#### 7.1.3 2<sup>nd</sup> Study - AR Representation of Cortical Thickness Results

The subjects included in this study are the same as the first study (table 7.1). Although the data is processed using a different software. Besides that, there is a need to establish a connection to send the results into the Unity environment. For that purpose, the Matlab was the chosen software.

### A. Data Processing

The data originated from the FreeSurfer extraction is divided in 4 groups, one for each cohort. In this study the CN cohort is also the control group, where the healthy subjects are located. For the 4 groups the average for the 66 regions (33 for each hemisphere) is calculated. Afterwards, between the healthy group and the other 3 cohorts (SMC, MCI, and AD) the ROIs are compared individually. Therefore, the result of the comparison is an array of 66 cortical thickness values one for each ROI. The array represent the thickness difference when comparing the ROIs of healthy subjects (CN) with the same regions found in the other cohorts (SMC, MCI, and AD). The array is then sent to the Unity system, the process is explained in the next section.

### B. Connection between Matlab & Unity

As mentioned before, the resulted values needed to be sent to Unity in order to be shown in the AR environment throughout the brain 3D model. Therefore, a TCP client was used to pass Matlab data into Unity.

The TCP client is a tool that enables the creation of client objects to communicate over TCP/IP (Transmission Control Protocol/Internet Protocol), allowing the connection between two or more objects. Hence, the two linked objects are the Matlab file and the C# file (attached to the ARCameraRig in Unity). Furthermore, the Matlab file works as a client that will send the data to the C# file that works as a server.

Having performed the connection, and since the 3D brain model has the meshes according to the resulted cortical thickness ROIs, the next step is to assign each ROI to the correspondent mesh. To see the different cortical thickness values in the 3D model a color gradient was used, where the minimum thickness value is represented in blue and the maximum in red.

## 7.2 AR development for AD study

In order to improve the interaction and immersion of the user in the AR environment, several objects were created. In the next sections these objects will be presented, with more detail given to the disease stages menu, since is the object where the user can manipulate and control the data to be shown on the 3D brain model.

### 7.2.1 Stages Menu

In figure 7.1 the AD stages menu is presented. In the menu, the user can find the 4 cohorts and also the loss bar button. The function of the menu is explained as a whole AR system in section 7.2.3.



Figure 7.1: Disease stages menu.

### 7.2.2 Loss Bar

The loss bar (figure 7.2) was created to give the user the capability to evaluate thickness loss in the ROIs. Hence the user can take conclusions concerning the cortical thickness evolution. The loss bar is activated when the user presses the corresponding button in the disease stages menu.

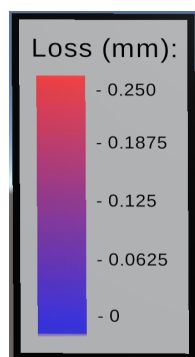


Figure 7.2: Loss bar.

### 7.2.3 AR system

To understand the different button/object interactions created to improve the AR user manipulation allied to the AD investigation study (section 7.1.3), figure 7.3 will be used as a guide.

Firstly, to access the disease menu the user needs to press the ON/OFF button bellow the 3D brain model (figure 7.3.a). When pressed, the menu appears (figure 7.3.b). Then, the user can select the AD disease, and activate the loss bar by using the corresponding button. In the disease stages menu (figure 7.3.c), the user has the capability to choose what comparison he wants to visualize, i.e. if the SMC button is pressed, the results of the comparison between CN and SMC will be shown as a gradient of colors in the 3D model. In figure 7.3.d the global AR system for the AD application is represented, with the comparison between the AD and CN cohorts.

For the purpose of better explaining the AR system, a set of three videos was recorded. The videos can be found in the following links:

- AR first person view with Leap Motion and SC sensors:

<https://youtu.be/vDCqBXOp-3M>

- AR with Leap Motion and SC sensors for AD research:

<https://youtu.be/yXMpcFGrRMY>

- AR tools applied to AD research, without SC Sensor:

<https://youtu.be/kJLFtH8mlXA>

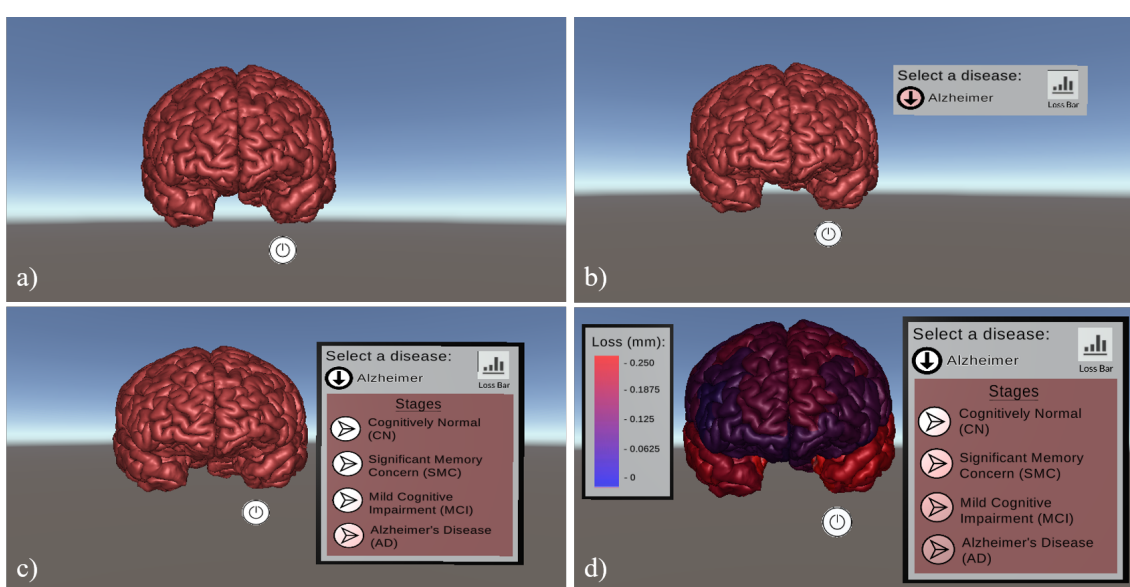


Figure 7.3: a) Model with On/Off button b) Disease menu c) Disease stages menu d) Loss bar.



# Chapter 8

## Results & Discussion

In this chapter, the results for the two studies conducted in this work are represented. In section 8.3, a discussion is done by comparing the results with the conclusions extracted from the two articles referenced in section 7.1. Hence, the quality of the results is evaluated in order to obtain the main goal of supporting the already proposed theories from the studies.

### 8.1 1<sup>st</sup> Study - ADNI Statistical Analysis

The results of the ADNI statistical analysis are represented in the present section. For each cohort, the ROIs' average and respective standard deviation was calculated. The process was performed for the two brain hemispheres. Therefore the results can be observed in tables B.1, B.2, B.3, and B.4. In table 8.1, the difference between the mean thickness at the ROIs means are presented, when comparing each of the SMC, MCI, and AD cohorts with the control group (CN).

Table 8.2 shows the percentage of thickness loss when compared the distinct cohorts with the control group.

When analyzing the mean results obtained for the SMC cohort with the results of the healthy patients (CN), there are a few differences, with the majority of the SMC ROIs being lower when compared with the same ROIs in the CN group for both hemispheres. The results are supported by data found in CN-SMC column of table 8.1 and 8.2, allowing to conclude that for each of the ROIs considered, the difference is inferior to 0.050 millimeters, for both hemispheres. A few exceptions are the caudal anterior cingulate, lateral orbital frontal, precentral, superior frontal, and temporal pole, over the 34 ROIs.

For the MCI group, the results show more thickness loss when compared to the same analysis of the SMC cohort, with more relevance to the ROIs that constitute the temporal lobe such as temporal pole, superior temporal, middle temporal, and entorhinal. The last one shows a mean difference higher than 0.200 millimeters which corresponds to a loss percentage higher than 6%, for both hemispheres.

Finally, the AD group describes the highest mean differences for the majority of the ROIs when compared with the other two cohorts analysis. This cohort also demonstrates the same behavior as the MCI cohort, in terms of temporal lobe atrophy. Besides that, it is clear that the CN-AD analysis shows differences between the results of each hemisphere, with the left hemisphere being the most damaged concerning the ROIs cortical thickness atrophy.

Table 8.1: Mean differences between the CN group and the other 3 cohorts (millimeters)

| Mean Differences           | CN-SMC |       | CN-MCI |       | CN-AD |       |
|----------------------------|--------|-------|--------|-------|-------|-------|
|                            | Left   | Right | Left   | Right | Left  | Right |
| Bank of Superior Temporal  | 0.045  | 0.009 | 0.077  | 0.045 | 0.164 | 0.144 |
| Caudal Anterior Cingulate  | 0.036  | 0.058 | 0.008  | 0.011 | 0.031 | 0.021 |
| Caudal Middle Frontal      | 0.038  | 0.029 | 0.060  | 0.053 | 0.138 | 0.126 |
| Cuneus                     | 0.006  | 0.009 | 0.011  | 0.000 | 0.042 | 0.043 |
| Entorhinal                 | 0.049  | 0.002 | 0.236  | 0.273 | 0.635 | 0.619 |
| Fusiform                   | 0.015  | 0.006 | 0.068  | 0.074 | 0.176 | 0.181 |
| Inferior Parietal          | 0.016  | 0.008 | 0.061  | 0.050 | 0.159 | 0.147 |
| Inferior Temporal          | 0.013  | 0.005 | 0.070  | 0.065 | 0.193 | 0.173 |
| Isthmus Cingulate          | 0.015  | 0.049 | 0.069  | 0.037 | 0.168 | 0.133 |
| Lateral Occipital          | 0.046  | 0.013 | 0.032  | 0.026 | 0.096 | 0.074 |
| Lateral Orbital Frontal    | 0.033  | 0.063 | 0.058  | 0.055 | 0.060 | 0.049 |
| Lingual                    | 0.016  | 0.036 | 0.037  | 0.056 | 0.065 | 0.090 |
| Medial Orbital Frontal     | 0.019  | 0.029 | 0.023  | 0.043 | 0.050 | 0.037 |
| Middle Temporal            | 0.037  | 0.039 | 0.095  | 0.081 | 0.221 | 0.199 |
| Parahippocampal            | 0.004  | 0.016 | 0.062  | 0.072 | 0.238 | 0.213 |
| Paracentral                | 0.016  | 0.036 | 0.021  | 0.045 | 0.054 | 0.070 |
| Pars Opercularis           | 0.013  | 0.010 | 0.054  | 0.049 | 0.055 | 0.088 |
| Pars Orbitalis             | 0.004  | 0.003 | 0.039  | 0.065 | 0.029 | 0.042 |
| Pars Triangularis          | 0.021  | 0.035 | 0.050  | 0.035 | 0.063 | 0.027 |
| Pericalcarine              | 0.044  | 0.005 | 0.002  | 0.003 | 0.020 | 0.027 |
| Postcentral                | 0.035  | 0.014 | 0.035  | 0.007 | 0.072 | 0.064 |
| Posterior Cingulate        | 0.016  | 0.010 | 0.038  | 0.016 | 0.102 | 0.017 |
| Precentral                 | 0.031  | 0.080 | 0.037  | 0.046 | 0.080 | 0.072 |
| Precuneus                  | 0.008  | 0.017 | 0.051  | 0.049 | 0.149 | 0.152 |
| Rostral Anterior Cingulate | 0.010  | 0.024 | 0.020  | 0.013 | 0.043 | 0.021 |
| Rostral Middle Frontal     | 0.030  | 0.043 | 0.049  | 0.036 | 0.068 | 0.054 |
| Superior Frontal           | 0.043  | 0.063 | 0.060  | 0.053 | 0.113 | 0.098 |
| Superior Parietal          | 0.040  | 0.049 | 0.051  | 0.060 | 0.122 | 0.134 |
| Superior Temporal          | 0.009  | 0.021 | 0.092  | 0.086 | 0.200 | 0.167 |
| Supramarginal              | 0.021  | 0.009 | 0.058  | 0.029 | 0.137 | 0.096 |
| Frontal Pole               | 0.009  | 0.040 | 0.014  | 0.022 | 0.007 | 0.075 |
| Temporal Pole              | 0.005  | 0.073 | 0.133  | 0.234 | 0.309 | 0.422 |
| Transverse Temporal        | 0.000  | 0.039 | 0.042  | 0.009 | 0.045 | 0.018 |
| Insula                     | 0.040  | 0.044 | 0.063  | 0.060 | 0.138 | 0.122 |

Table 8.2: Mean differences (%) between the CN group and the other 3 cohorts

| Mean Differences           | CN-SMC |       | CN-MCI |       | CN-AD |       |
|----------------------------|--------|-------|--------|-------|-------|-------|
|                            | Left   | Right | Left   | Right | Left  | Right |
| Bank of Superior Temporal  | 1.87   | 0.36  | 3.20   | 1.82  | 6.80  | 5.82  |
| Caudal Anterior Cingulate  | 1.39   | 2.38  | 0.31   | 0.45  | 1.20  | 0.86  |
| Caudal Middle Frontal      | 1.56   | 1.20  | 2.46   | 2.20  | 5.66  | 5.22  |
| Cuneus                     | 0.32   | 0.47  | 0.59   | 0.00  | 2.24  | 2.26  |
| Entorhinal                 | 1.44   | 0.06  | 6.95   | 7.78  | 18.71 | 17.64 |
| Fusiform                   | 0.56   | 0.22  | 2.54   | 2.72  | 6.57  | 6.66  |
| Inferior Parietal          | 0.69   | 0.34  | 2.62   | 2.13  | 6.84  | 6.26  |
| Inferior Temporal          | 0.48   | 0.18  | 2.58   | 2.37  | 7.11  | 6.32  |
| Isthmus Cingulate          | 0.65   | 2.10  | 2.97   | 1.58  | 7.23  | 5.69  |
| Lateral Occipital          | 2.12   | 0.59  | 1.47   | 1.17  | 4.42  | 3.33  |
| Lateral Orbital Frontal    | 1.28   | 2.48  | 2.26   | 2.16  | 2.33  | 1.93  |
| Lingual                    | 0.79   | 1.73  | 1.83   | 2.70  | 3.21  | 4.34  |
| Medial Orbital Frontal     | 0.81   | 1.23  | 0.99   | 1.82  | 2.14  | 1.57  |
| Middle Temporal            | 1.34   | 1.40  | 3.44   | 2.91  | 8.00  | 7.15  |
| Parahippocampal            | 0.14   | 0.59  | 2.24   | 2.64  | 8.60  | 7.82  |
| Paracentral                | 0.69   | 1.52  | 0.90   | 1.90  | 2.32  | 2.95  |
| Pars Opercularis           | 0.53   | 0.40  | 2.18   | 1.97  | 2.22  | 3.54  |
| Pars Orbitalis             | 0.15   | 0.12  | 1.51   | 2.50  | 1.12  | 1.62  |
| Pars Triangularis          | 0.90   | 1.49  | 2.13   | 1.49  | 2.69  | 1.15  |
| Pericalcarine              | 2.70   | 0.30  | 0.12   | 0.18  | 1.23  | 1.64  |
| Postcentral                | 1.72   | 0.70  | 1.72   | 0.35  | 3.53  | 3.20  |
| Posterior Cingulate        | 0.67   | 0.43  | 1.59   | 0.69  | 4.27  | 0.73  |
| Precentral                 | 1.25   | 3.26  | 1.49   | 1.88  | 3.22  | 2.94  |
| Precuneus                  | 0.35   | 0.74  | 2.23   | 2.12  | 6.53  | 6.58  |
| Rostral Anterior Cingulate | 0.37   | 0.86  | 0.75   | 0.46  | 1.61  | 0.75  |
| Rostral Middle Frontal     | 1.32   | 1.90  | 2.16   | 1.59  | 3.00  | 2.39  |
| Superior Frontal           | 1.69   | 2.49  | 2.36   | 2.09  | 4.45  | 3.87  |
| Superior Parietal          | 1.87   | 2.29  | 2.39   | 2.80  | 5.72  | 6.26  |
| Superior Temporal          | 0.34   | 0.79  | 3.47   | 3.23  | 7.55  | 6.27  |
| Supramarginal              | 0.87   | 0.38  | 2.40   | 1.21  | 5.67  | 4.00  |
| Frontal Pole               | 0.34   | 1.53  | 0.53   | 0.84  | 0.27  | 2.87  |
| Temporal Pole              | 0.14   | 1.96  | 3.74   | 6.29  | 8.69  | 11.34 |
| Transverse Temporal        | 0.00   | 1.73  | 1.85   | 0.40  | 1.98  | 0.80  |
| Insula                     | 1.40   | 1.54  | 2.21   | 2.10  | 4.83  | 4.27  |

## 8.2 2<sup>nd</sup> Study - AR Representation of Cortical Thickness Results

Table 8.3 illustrates the results of cortical thickness difference for the three comparison analysis. For each ROI, a color concerning the respective ROI value was attributed. Hence the colored 3D model maps are formed, and the user can conclude about the brain cortical thickness atrophy.

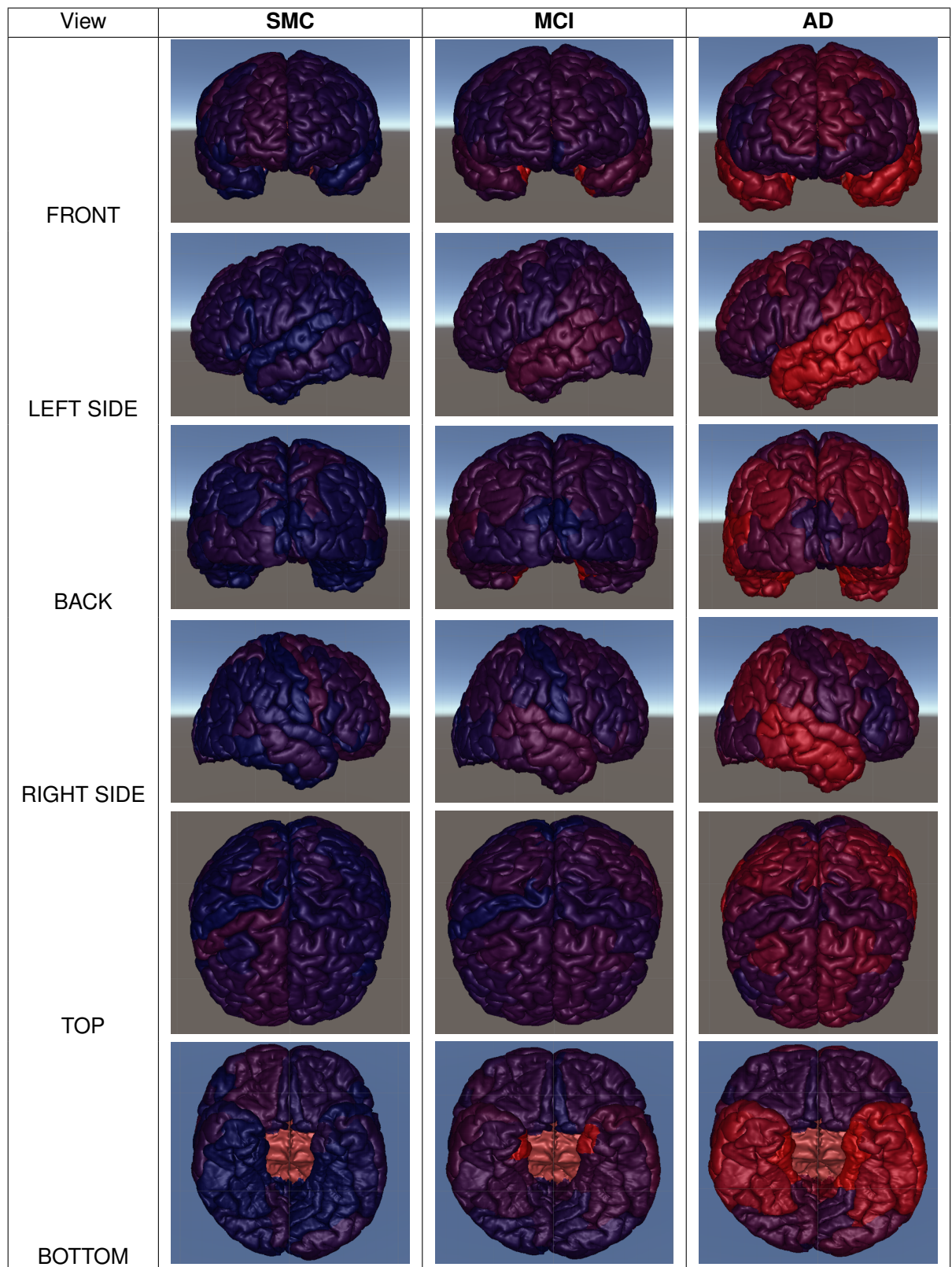
For the overall ROIs in SMC analysis, the predominant color is blue, with some glimpses of purple. As blue and purple mean low damage to the cortex, the SMC patients show, in average, few alterations to the brain cortex when compared with healthy patients.

The MCI analysis starts to reveal a slight difference in the ROIs related to the temporal lobe, as shown in the left and right side view in table 8.3. Besides that, note that the entorhinal ROI has a red color for the two hemispheres, which means high cortical thickness damage.

The AD analysis demonstrates the same atrophy evolution on the temporal lobe, in ROIs such as superior temporal, inferior temporal, middle temporal, fusiform, entorhinal, and parahippocampal. Note that the phenomenon is visualized in both hemispheres. When looking at the back view, it is clear that the precuneus, supramarginal, superior, and inferior ROIs included in the parietal lobe are also very affected. The frontal lobe, in specific the superior and caudal middle ROIs, suffers some damage as well, however it is not so predominant as the atrophy observed in the parietal and frontal lobes.

In general, when comparing the results for the three cohorts, SMC shows the lowest atrophy. On the other side, the AD results represent a high brain cortical thickness damage, demonstrating an atrophy evolution of what is seen in the MCI analysis, specifically in the temporal lobe.

Table 8.3: Cortical thickness results for the three cohorts



### 8.3 Discussion

This section will be used to discuss the interconnection between the two studies' results supported by the main conclusions from articles ([63][64]).

According to Li, Chuanming *et al.* [63], the cortical thickness suffered atrophy for the majority of the ROIs, with the MCI group showing cortical thickness to be between the CN group and the AD group. As referred in section 8.1, this process is also observed and the same behavior is illustrated by table 8.3, where it is possible to see that the AD brain is more affected by tissue loss than the SMC, MCI and CN groups.

In their work, Lehmann, Manja *et al.* [64], explained that when comparing AD with control patients, the cortical thickness was thinnest for the temporal lobe, followed by the parietal lobe. This result was also presented in section 8.1, and the 3D brain model shows the same results (figure 8.1). Therefore, such conclusion is fully supported by the results obtained in our work.

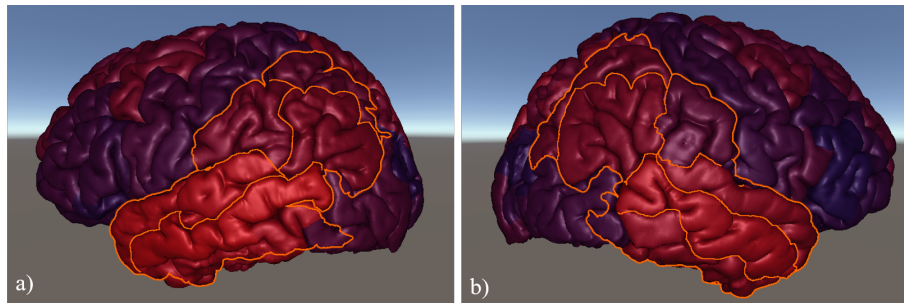


Figure 8.1: AD analysis with temporal and parietal lobes marked: a) Left view b) Right view.

The same author report that the entorhinal region showed the biggest loss of cortical thickness. When compared with the mean differences in table 8.1, the entorhinal ROI is the most affected with 0.236 and 0.273 millimeters of thickness loss for left and right hemisphere, respectively. The same behavior occurs in the AD analysis with 0.635 and 0.619 millimeters for the left and right hemispheres, respectively. The results of the second study also show predominant cortical thickness atrophy of the entorhinal cortex for the MCI and AD analysis, observed in figure 8.2.

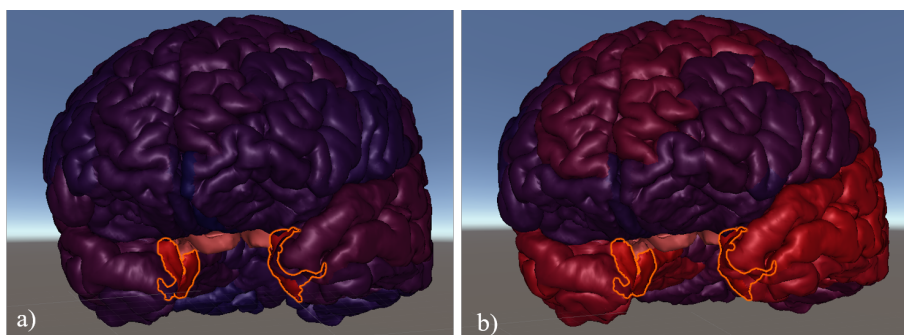


Figure 8.2: Entorhinal ROI for a) MCI analysis b) AD analysis.

Lehmann also explains that the left hemisphere is more affected than the right; this conclusion was also obtained in section 8.1, as supported by the CN-AD column of table 8.1.



# Chapter 9

## Conclusions

The objective of this dissertation work was to develop an AR technology capable of aiding AD research. Thereby, the user is able to see and manipulate a 3D brain model with the possibility to discriminate different cortical thickness losses, while comparing the cohort analysis, for the distinct ROIs in the 3D brain model.

For AR development, the NS project was used as the main foundation. Therefore, the Leap Motion sensor allowed the interaction between the user and the created VE. The other main component of the work was the implementation of the SC sensor, establishing depth perception, and improving the user immersion into the AR environment. After achieving an efficient and stable AR system, with the user capable of manipulating the 3D models, the project was conducted to reach the main goal of creating a AR based tool to aid the AD research.

A communication system between Matlab and Unity was developed, with Matlab accessing and processing data from ADNI MRI's database and sending it to Unity through a TCP/IP connection tool. With this method, Unity was able to receive and assign the processed cortical thickness data for each ROI cohort analysis.

Such results support the conclusions reached by Li, Chuanming *et al.* [63] and Lehmann, Manja *et al.* [64]. Besides that, it's possible to verify the same cortical thickness atrophy results for each ROI, when performing the AR immersion. Since the user is capable of, in the 3D brain model, discriminates each ROI area, this allows the user to have a sophisticated view of the cortical thickness damage for each ROI.

This technology allows the user to interact physically with the virtual objects. Since the objects can be manipulated, rotated, the user can take other conclusions about the evolution of the disease that he would not be able to, just by analyzing a set of MRI's. Therefore, the technology has a research application, even though it can also be used as an interactive way to teach and learn, i.e. acquire knowledge about the evolution of the disease.

Throughout the work, some difficulties were felted, such as the implementation of the SC sensor. Since it is a relatively new sensor, the information related to the application of the sensor

to AR environments is almost nonexistent. Another step back was related to the communication between Unity and Matlab, as the tool used, in spite of being efficient to the dissertation objectives, it's not very user friendly and requires time to understand how it works.

In general, the main objectives of the dissertation were accomplished. AR technology has a huge versatility in terms of the study of other diseases. All the technologies and strategies developed, can in principle, be applied to other fields of medicine. The final application can be tailored for both pedagogical and research purposes. The work was mainly focused on the analysis of cortical thickness, but besides that, the system can be used to research other types of features such as ROIs volume and area, etc.

# **Chapter 10**

## **Future Work**

In this dissertation, the application of an AR tool for AD research was created. As mentioned in section 3.2, AR creates an environment where the sense of the virtual world is mixed with the real-world environment. This allows the use of the technology in a large range of domains.

Having accomplished a stable and efficient connection between the Unity software and Matlab, the software is capable to access any database with the right features. With this in mind, other measures besides the cortical thickness can be evaluated and observed in the AR environment. Note that, for example, having a group of healthy patients, the researcher can generate a set of normal measures, and evaluate for each new patient the deviation from normality of the brain cortical thickness measures.

There are some features of the work that can be improved, such as the connection between Matlab and Unity. Since it uses the TCP/IP tool, the connection is limited and the data transmission can only be performed in one direction at a time. In other words, when the AR system is activated, the tool can only perform the transmission of data from the Matlab to Unity or vice versa. Therefore, a future technology should consider the use of another tool to establish the connection. Another important aspect is the NS headset used. Being the headset the main child of a new project, its configuration is based on tests and ideas shared by researchers. Hence, the headset still has room to improve in terms of structure and functionality.

The developed AR system can be applied to other fields of study such as pedagogy. Since it uses realistic 3D brain and skull models, the technology can be used by teachers to educate the students about AD evolution from SMC to AD patients.

To sum up, the AR technology has infinite applications potentially useful to the society, with special interest to the healthcare and disease research sectors.



# References

- [1] Jonathan Steuer. Defining virtual reality: Characteristics determining telepresence. *Journal of Communication*, 42(4):73–94, 1992.
- [2] F.P. Brooks. What’s Real About Virtual Reality? (December):2–3, 2005.
- [3] John R. Wilson. Virtual environments and ergonomics: Needs and opportunities. *Ergonomics*, 40(10):1057–1077, 1997.
- [4] P Milgram, H Takemura, a Utsumi, and F Kishino. Mixed Reality ( MR ) Reality-Virtuality ( RV ) Continuum. *Systems Research*, 2351(Telemanipulator and Telepresence Technologies):282–292, 1994.
- [5] A. C. Boud, D. J. Haniff, C. Baber, and S. J. Steiner. Virtual reality and augmented reality as a training tool for assembly tasks. *Proceedings of the International Conference on Information Visualisation*, 1999-January:32–36, 1999.
- [6] Clifford R. Jack, David S. Knopman, William J. Jagust, Leslie M. Shaw, Paul S. Aisen, Michael W. Weiner, Ronald C. Petersen, and John Q. Trojanowski. Hypothetical model of dynamic biomarkers of the Alzheimer’s pathological cascade. *The Lancet Neurology*, 9(1):119–128, 2010.
- [7] The Medical Futurist. Augmented reality in healthcare will be revolutionary: 9 examples. <https://medicalfuturist.com/augmented-reality-in-healthcare-will-be-revolutionary/>. Accessed: 2020-02.
- [8] Jennifer Herron. Augmented reality in medical education and training. *Journal of Electronic Resources in Medical Libraries*, 13(2):51–55, 2016.
- [9] Alzheimer’s Association. 2019 Alzheimer’s disease facts and figures. *Alzheimer’s & Dementia*, 15(3):321–387, 2019.
- [10] Paul Rookes and Jane Willson. *Perception*, volume 53. 2018.
- [11] D. V.S.X. De Silva, E. Ekmekcioglu, W. A.C. Fernando, and S. T. Worrall. Display dependent preprocessing of depth maps based on just noticeable depth difference modeling. *IEEE Journal on Selected Topics in Signal Processing*, 5(2):335–351, 2011.

- [12] Nestor Matthews, Xin Meng, Peng Xu, and Ning Qian. A physiological theory of depth perception from vertical disparity. *Vision Research*, 43(1):85–99, 2003.
- [13] Congrès international de médecine du travail (15 ; 1966 ; Vienne). *Physiology psychology*. 2003.
- [14] Lidar, Precision is Key. <https://ecko360industrial.com/services/lidar/>. Accessed: 2019-11.
- [15] Brent Schwarz. Lidar: Mapping the world in 3D. *Nature Photonics*, 4(7):429–430, 2010.
- [16] S Crutchley. The Light Fantastic: Using airborne lidar in archaeological survey. *ISPRS TC VII Symposium – 100 Years ISPRS*, XXXVIII(July):160–164, 2010.
- [17] Rajeev Thakur. Scanning LIDAR in advanced driver assistance systems and beyond. *IEEE Consumer Electronics Magazine*, 5(3):48–54, 2016.
- [18] Mathieu Dassot, Thiéry Constant, and Meriem Fournier. The use of terrestrial LiDAR technology in forest science: Application fields, benefits and challenges. *Annals of Forest Science*, 68(5):959–974, 2011.
- [19] Jamaliah Abdul Majid et al. A Brief History of LiDAR. *Acta Universitatis Agriculturae et Silviculturae Mendelianae Brunensis*, 16(2):39–55, 2015.
- [20] Cyril Vienne, Justin Plantier, Pascaline Neveu, and Anne Emmanuelle Priot. The role of vertical disparity in distance and depth perception as revealed by different stereo-camera configurations. *i-Perception*, 7(6), 2016.
- [21] Larry Li. Time-of-Flight Camera—An Introduction. *Texas Instruments - Technical White Paper*, (January):10, 2014.
- [22] Marvin Lindner, Ingo Schiller, Andreas Kolb, and Reinhard Koch. Time-of-Flight sensor calibration for accurate range sensing. *Computer Vision and Image Understanding*, 114(12):1318–1328, 2010.
- [23] Eugen Baumgart and Ulrich Kubitscheck. Scanned light sheet microscopy with confocal slit detection. *Optics Express*, 20(19):21805, 2012.
- [24] D Khadraoui, G Motyl, P Martinet, J Gallice, F Chaumette, and I Introduction. Visual Servoing in Robotics Scheme Using a Cameraaser-Stripe Sensor. 12(5), 1996.
- [25] Horng Hai Loh and Ming Sing Lu. Printed circuit board inspection using image analysis. *IEEE Transactions on Industry Applications*, 35(2):426–432, 1999.
- [26] Nathan Silberman and Rob Fergus. Indoor Scene Segmentation using a Structured Light Sensor. pages 601–608, 2011.

- [27] Matjaž Mihelj, Domen Novak, and Samo Beguš. *Virtual Reality Technology and Applications*, volume 68. 2014.
- [28] Grigore C. Burdea; Philippe Coiffet. *Virtual Reality technology*. John Wiley & Sons, Inc., second edition edition, 2003.
- [29] Carly A Kocurek. The treachery of pixels : Reconsidering feelies in an era of digital play. 5(3):295–306, 2013.
- [30] Stanley G. Weinbaum. *Pygmalion's Spectacles*. Floating Press, 1949.
- [31] Morton L. Heilig. Sensorama simulator, January 1961. US3050870A.
- [32] Wikipedia Contributors. Cave Automatic Virtual Environment. [https://en.wikipedia.org/w/index.php?title=Cave\\_automatic\\_virtual\\_environment&oldid=929407531](https://en.wikipedia.org/w/index.php?title=Cave_automatic_virtual_environment&oldid=929407531). Accessed: 2019-11.
- [33] John Vince. *10 Virtual Reality Techniques in Flight Simulation*. ACADEMIC PRESS LIMITED, 1993.
- [34] Wikipedia Contributors. Driving Simulator. [https://en.wikipedia.org/w/index.php?title=Driving\\_simulator&oldid=934644966](https://en.wikipedia.org/w/index.php?title=Driving_simulator&oldid=934644966). Accessed: 2020-01.
- [35] Wikipedia Contributors. Flight Simulator. [https://en.wikipedia.org/w/index.php?title=Flight\\_simulator&oldid=925868794](https://en.wikipedia.org/w/index.php?title=Flight_simulator&oldid=925868794). Accessed: 2020-01.
- [36] Heidi Sveistrup. Motor rehabilitation using virtual reality. 8:1–8, 2004.
- [37] Bob G. Witmer and Michael J. Singer. Measuring presence in virtual environments: A presence questionnaire. *Presence: Teleoperators and Virtual Environments*, 7(3):225–240, 1998.
- [38] Grigore C. Burdea. Haptic feedback for virtual reality. (June), 1999.
- [39] Jean Vertut and Philippe Coiffet. Robot technology. vol. 3a. teleoperation and robotics: evolution and development, Jan 1985.
- [40] A M Okamura. Methods for haptic feedback in teleoperated robot-assisted surgery. 31(6):499–508, 2004.
- [41] Steven Feiner. Knowledge-Based Augmented Reality. (July), 1993.
- [42] S. Zlatanova. *Augmented reality technology applications*, volume 17. 2002.
- [43] Oliver Bimber and Ramesh Raskar. *Spatial Augmented Reality*, volume 2005. 2005.
- [44] Ivan E. Sutherland. A head-mounted three dimensional display. In *Proceedings of the December 9-11, 1968, Fall Joint Computer Conference, Part I*, AFIPS '68 (Fall, part I), page 757–764, New York, NY, USA, 1968. Association for Computing Machinery.

- [45] T.P. Caudell and D.W. Mizell. Augmented reality: an application of heads-up display technology to manual manufacturing processes. pages 659–669 vol.2, 2003.
- [46] Exploring MARS: Developing indoor and outdoor user interfaces to a mobile augmented reality system. *Computers and Graphics (Pergamon)*, 23(6):779–785, 1999.
- [47] Hirokazu Kato and Mark Billinghurst. Marker Tracking and HMD Calibration for a Video-based Augmented Reality Conferencing System. 1999.
- [48] Jim Vallino. Introduction to Augmented Reality. <http://www.se.rit.edu/~jrv/research/ar/introduction.html>. Accessed: 2020-01.
- [49] William E Lorensen, General Electric, Christopher Nafis, General Electric, and Ron Kikinis. Enhancing Reality in the Operating Room. (May 2014), 1996.
- [50] Andrei State, David T Chen, Chris Tector, Andrew Brandt, Hong Chen, Ryutarou Ohbuchi, Mike Bajura, and Henry Fuchs. Case Study : Observing a Volume Rendered Fetus Within a Pregnant Patient Case Study : Observing a Volume Rendered Fetus within a Pregnant Patient. 1994.
- [51] M Kasim and A Jalil. Overview of Virtual Reality in Science and Engineering. pages 7–30.
- [52] J W S Chong, S K Ong, A Y C Nee, and K Youcef-youmi. Robotics and Computer-Integrated Manufacturing Robot programming using augmented reality : An interactive method for planning collision-free paths. 25:689–701, 2009.
- [53] Francesca De Crescenzo, Massimiliano Fantini, Franco Persiani, Luigi Di Stefano, Pietro Azzari, and Samuele Salti. Augmented Reality for Aircraft Maintenance Training and Operations Support. 2011.
- [54] Dave Sims. New Realities in Aircraft Design and Manufacture. (March):1994, 1994.
- [55] Ultraleap. *Leap Motion Controller - The world ' s leading hand tracking technology*, 2019.
- [56] Leap Motion / Developer. Project north star. <https://developer.leapmotion.com/northstar>. Accessed: 2020-03.
- [57] H. Niu, I. Álvarez-Álvarez, F. Guillén-Grima, and I. Aguinaga-Ontoso. Prevalencia e incidencia de la enfermedad de Alzheimer en Europa: metaanálisis. *Neurologia*, 32(8):523–532, 2017.
- [58] Martin Prince, Renata Bryce, Emiliano Albanese, Anders Wimo, Wagner Ribeiro, and Cleusa P. Ferri. The global prevalence of dementia: A systematic review and metaanalysis. *Alzheimer's and Dementia*, 9(1):63–75.e2, 2013.
- [59] Martin Prince and Jim Jackson. World Alzheimer Report 2009. *Alzheimer's Disease International*, pages 1–96, 2009.

- [60] G. Lucotte, S. Visvikis, B. Leininger-Muler, F. David, S. Berriche, S. Reveilleau, R. Couderc, M. C. Babron, D. Aguillon, and G. Siest. Association of apolipoprotein E allele  $\epsilon$ 4 with late-onset sporadic Alzheimer's disease. *American Journal of Medical Genetics*, 54(3):286–288, 1994.
- [61] N T Lautenschlager, L A Cupples, V S Rao, S A Auerbach, R Becker, R Jones, H Karlinsky, W A Kukull, A Kurz, E B Larson, J H Growdon, L A Farrer, and P D. Risk of dementia among relatives of Alzheimer ' s disease patients in the MIRAGE study : What is in store for the oldest old ? 6781, 1996.
- [62] Bradley T. Wyman, Danielle J. Harvey, Karen Crawford, Matt A. Bernstein, Owen Carmichael, Patricia E. Cole, Paul K. Crane, Charles Decarli, Nick C. Fox, Jeffrey L. Gunter, Derek Hill, Ronald J. Killiany, Chahin Pachai, Adam J. Schwarz, Norbert Schuff, Matthew L. Senjem, Joyce Suhy, Paul M. Thompson, Michael Weiner, and Clifford R. Jack. Standardization of analysis sets for reporting results from ADNI MRI data. *Alzheimer's and Dementia*, 9(3):332–337, 2013.
- [63] Chuanming Li, Jian Wang, Li Gui, Jian Zheng, Chen Liu, and Hanjian Du. Alterations of whole-brain cortical area and thickness in mild cognitive impairment and alzheimer's disease. *Journal of Alzheimer's Disease*, 27(2):281–290, 2011.
- [64] Manja Lehmann, Sebastian J. Crutch, Gerard R. Ridgway, Basil H. Ridha, Josephine Barnes, Elizabeth K. Warrington, Martin N. Rossor, and Nick C. Fox. Cortical thickness and voxel-based morphometry in posterior cortical atrophy and typical Alzheimer's disease. *Neurobiology of Aging*, 32(8):1466–1476, 2011.
- [65] Michael W. Weiner, Paul S. Aisen, Clifford R. Jack, William J. Jagust, John Q. Trojanowski, Leslie Shaw, Andrew J. Saykin, John C. Morris, Nigel Cairns, Laurel A. Beckett, Arthur Toga, Robert Green, Sarah Walter, Holly Soares, Peter Snyder, Eric Siemers, William Potter, Patricia E. Cole, and Mark Schmidt. The Alzheimer's Disease Neuroimaging Initiative: Progress report and future plans. *Alzheimer's and Dementia*, 6(3):202–211.e7, 2010.
- [66] Chatchawan Rattanabannakit, Shannon L. Risacher, Sujuan Gao, Kathleen A. Lane, Steven A. Brown, Brenna C. McDonald, Frederick W. Unverzagt, Liana G. Apostolova, Andrew J. Saykin, and Martin R. Farlow. The cognitive change index as a measure of self and informant perception of cognitive decline: Relation to neuropsychological tests. *Journal of Alzheimer's Disease*, 51(4):1145–1155, 2016.
- [67] Cecily G. Swinford, Shannon L. Risacher, Arnaud Charil, Adam J. Schwarz, and Andrew J. Saykin. Memory concerns in the early Alzheimer's disease prodrome: Regional association with tau deposition. *Alzheimer's and Dementia: Diagnosis, Assessment and Disease Monitoring*, 10(March):322–331, 2018.

- [68] Sid E. O'Bryant, Stephen C. Waring, C. Munro Cullum, James Hall, Laura Lacritz, Paul J. Massman, Philip J. Lupo, Joan S. Reisch, and Rachelle Doody. Staging dementia using clinical dementia rating scale sum of boxes scores: A Texas Alzheimer's research consortium study. *Archives of Neurology*, 65(8):1091–1095, 2008.
- [69] Ronald C. Petersen, Glenn E. Smith, Stephen C. Waring, Robert J. Ivnik, Eric G. Tangalos, and Emre Kokmen. Mild Cognitive Impairment: Clinical Characterization and Outcome. *Archives of Neurology*, 56(3):303–308, 03 1999.
- [70] Kimberly R. Chapman, Hanaan Bing-Canar, Michael L. Alosco, Eric G. Steinberg, Brett Martin, Christine Chaisson, Neil Kowall, Yorghos Tripodis, and Robert A. Stern. Mini Mental State Examination and Logical Memory scores for entry into Alzheimer's disease trials. *Alzheimer's Research and Therapy*, 8(1):1–11, 2016.
- [71] Rahul S. Desikan, Florent Ségonne, Bruce Fischl, Brian T. Quinn, Bradford C. Dickerson, Deborah Blacker, Randy L. Buckner, Anders M. Dale, R. Paul Maguire, Bradley T. Hyman, Marilyn S. Albert, and Ronald J. Killiany. An automated labeling system for subdividing the human cerebral cortex on MRI scans into gyral based regions of interest. *NeuroImage*, 31(3):968–980, 2006.
- [72] C. Chayer and M. Freedman. Frontal lobe functions. *Current neurology and neuroscience reports*, 1(6):547–552, 2001.
- [73] Queensland Brain Institute. Lobes of the brain. <https://qbi.uq.edu.au/brain/brain-anatomy/lobes-brain>. Accessed: 2020-04.
- [74] Pietro Zanuttigh, Giulio Marin, Carlo Dal Mutto, Fabio Dominio, Ludovico Minto, and Guido Maria Cortelazzo. *Time-of-Flight and Structured Light Depth Cameras*. 2016.
- [75] Inc. Occipital. Specs. <https://structure.io/structure-core/specs>. Accessed: 2020-02.
- [76] Fabian Hoflinger, Jorg Muller, Rui Zhang, Leonhard M. Reindl, and Wolfram Burgard. A wireless micro inertial measurement unit (IMU). *IEEE Transactions on Instrumentation and Measurement*, 62(9):2583–2595, 2013.
- [77] Projectnorthstar. <https://github.com/leapmotion/ProjectNorthStar/tree/master/Software>. Accessed: 2020-02.
- [78] Leap Motion. Unity modules leap motion's unity sdk 4.5.0. <https://github.com/UnityModules/core.html>. Accessed: 2020-03.
- [79] Mystery skull 1 & 2. <https://sketchfab.com/3d-models/mystery-skull-1-2-81e11000c8644beb99714884afb3b940>. Accessed: 2020-03.

- [80] Creative Commons. Attribution-sharealike 3.0 unported (cc by-sa 3.0). [https://creativecommons.org/licenses/by-sa/3.0/deed.en\\_GB](https://creativecommons.org/licenses/by-sa/3.0/deed.en_GB). Accessed: 2020-05.
- [81] Anderson Winkler. Brain for blender. <https://brainder.org/research/brain-for-blender/>. Accessed: 2020-05.
- [82] Freesurfer. <http://surfer.nmr.mgh.harvard.edu>. Accessed: 2020-04.
- [83] Anders M Dale, Bruce Fischl, and Martin I Sereno. Cortical Surface-Based Analysis. II. Inflation, Flattening, and a Surface-Based Coordinate System. *NeuroImage*, 9(2):179–194, 1999.
- [84] B Fischl, M I Sereno, and A M Dale. Cortical surface-based analysis. I. Segmentation and Surface Reconstruction. *NeuroImage*, 9(2):195–207, 1999.
- [85] Bruce Fischl, Arthur Liu, and Anders M. Dale. Automated manifold surgery: Constructing geometrically accurate and topologically correct models of the human cerebral cortex. *IEEE Transactions on Medical Imaging*, 20(1):70–80, 2001.
- [86] Eric Westman, Andrew Simmons, J. Sebastian Muehlboeck, Patrizia Mecocci, Bruno Vellas, Magda Tsolaki, Iwona Kloszewska, Hilkka Soininen, Michael W. Weiner, Simon Lovestone, Christian Spenger, and Lars Olof Wahlund. AddNeuroMed and ADNI: Similar patterns of Alzheimer’s atrophy and automated MRI classification accuracy in Europe and North America. *NeuroImage*, 58(3):818–828, 2011.



## **Appendix A**

### **Recorded Videos**

The links for the videos recorded to aid the understanding of the technology by the reader are also listed here.

- Augmented Reality first person view with Leap Motion and Structure Core sensors:  
<https://youtu.be/vDCqBXOp-3M>
- Augmented Reality with Leap Motion and Structure Core sensors for Alzheimer Disease research:  
<https://youtu.be/yXMpcFGrMY>
- Augmented Reality Tools applied to Alzheimer's Disease Research, Without Structure Core Sensor:  
<https://youtu.be/kJLFtH8mlXA>



## **Appendix B**

### **Tables - Chapter 8**

This appendix contains the tables with numerical results discussed in chapter 8.

Table B.1: Cortical thickness in CN group (mean and standard deviation, millimeters)

| ROIs                       | CN          |       |              |       |
|----------------------------|-------------|-------|--------------|-------|
|                            | <i>Left</i> |       | <i>Right</i> |       |
|                            | Mean        | S.D.  | Mean         | S.D.  |
| Bank of Superior Temporal  | 2.410       | 0.024 | 2.474        | 0.024 |
| Caudal Anterior Cingulate  | 2.587       | 0.039 | 2.434        | 0.037 |
| Caudal Middle Frontal      | 2.439       | 0.020 | 2.412        | 0.021 |
| Cuneus                     | 1.872       | 0.018 | 1.904        | 0.021 |
| Entorhinal                 | 3.394       | 0.056 | 3.509        | 0.062 |
| Fusiform                   | 2.678       | 0.024 | 2.716        | 0.025 |
| Inferior Parietal          | 2.324       | 0.021 | 2.348        | 0.021 |
| Inferior Temporal          | 2.716       | 0.026 | 2.737        | 0.023 |
| Isthmus Cingulate          | 2.325       | 0.029 | 2.337        | 0.031 |
| Lateral Occipital          | 2.171       | 0.020 | 2.221        | 0.020 |
| Lateral Orbital Frontal    | 2.571       | 0.021 | 2.543        | 0.021 |
| Lingual                    | 2.022       | 0.019 | 2.075        | 0.019 |
| Medial Orbital Frontal     | 2.332       | 0.022 | 2.362        | 0.023 |
| Middle Temporal            | 2.762       | 0.024 | 2.783        | 0.022 |
| Parahippocampal            | 2.766       | 0.044 | 2.723        | 0.038 |
| Paracentral                | 2.325       | 0.020 | 2.371        | 0.021 |
| Pars Opercularis           | 2.472       | 0.019 | 2.486        | 0.021 |
| Pars Orbitalis             | 2.587       | 0.027 | 2.597        | 0.026 |
| Pars Triangularis          | 2.346       | 0.020 | 2.342        | 0.020 |
| Pericalcarine              | 1.632       | 0.020 | 1.650        | 0.020 |
| Postcentral                | 2.038       | 0.017 | 2.000        | 0.018 |
| Posterior Cingulate        | 2.391       | 0.025 | 2.316        | 0.027 |
| Precentral                 | 2.483       | 0.019 | 2.453        | 0.021 |
| Precuneus                  | 2.282       | 0.020 | 2.311        | 0.019 |
| Rostral Anterior Cingulate | 2.673       | 0.033 | 2.798        | 0.037 |
| Rostral Middle Frontal     | 2.270       | 0.017 | 2.260        | 0.018 |
| Superior Frontal           | 2.539       | 0.019 | 2.531        | 0.019 |
| Superior Parietal          | 2.134       | 0.020 | 2.140        | 0.021 |
| Superior Temporal          | 2.649       | 0.024 | 2.662        | 0.023 |
| Supramarginal              | 2.417       | 0.019 | 2.399        | 0.020 |
| Frontal Pole               | 2.625       | 0.035 | 2.611        | 0.037 |
| Temporal Pole              | 3.555       | 0.050 | 3.720        | 0.051 |
| Transverse Temporal        | 2.273       | 0.031 | 2.259        | 0.034 |
| Insula                     | 2.856       | 0.026 | 2.854        | 0.027 |

Table B.2: Cortical thickness in SMC group (mean and standard deviation, millimeters)

| ROIs                       | SMC         |       |              |       |
|----------------------------|-------------|-------|--------------|-------|
|                            | <i>Left</i> |       | <i>Right</i> |       |
|                            | Mean        | S.D.  | Mean         | S.D.  |
| Bank of Superior Temporal  | 2.365       | 0.032 | 2.465        | 0.032 |
| Caudal Anterior Cingulate  | 2.551       | 0.053 | 2.376        | 0.049 |
| Caudal Middle Frontal      | 2.401       | 0.027 | 2.383        | 0.028 |
| Cuneus                     | 1.878       | 0.024 | 1.913        | 0.028 |
| Entorhinal                 | 3.345       | 0.075 | 3.511        | 0.084 |
| Fusiform                   | 2.693       | 0.032 | 2.722        | 0.034 |
| Inferior Parietal          | 2.308       | 0.029 | 2.340        | 0.028 |
| Inferior Temporal          | 2.703       | 0.035 | 2.742        | 0.030 |
| Isthmus Cingulate          | 2.340       | 0.039 | 2.386        | 0.042 |
| Lateral Occipital          | 2.125       | 0.026 | 2.208        | 0.027 |
| Lateral Orbital Frontal    | 2.538       | 0.028 | 2.480        | 0.028 |
| Lingual                    | 2.038       | 0.025 | 2.039        | 0.025 |
| Medial Orbital Frontal     | 2.313       | 0.030 | 2.333        | 0.031 |
| Middle Temporal            | 2.725       | 0.033 | 2.744        | 0.030 |
| Parahippocampal            | 2.762       | 0.059 | 2.739        | 0.051 |
| Paracentral                | 2.309       | 0.027 | 2.335        | 0.029 |
| Pars Opercularis           | 2.485       | 0.025 | 2.476        | 0.029 |
| Pars Orbitalis             | 2.591       | 0.036 | 2.594        | 0.034 |
| Pars Triangularis          | 2.325       | 0.026 | 2.307        | 0.028 |
| Pericalcarine              | 1.676       | 0.027 | 1.645        | 0.026 |
| Postcentral                | 2.003       | 0.023 | 2.014        | 0.024 |
| Posterior Cingulate        | 2.375       | 0.033 | 2.326        | 0.036 |
| Precentral                 | 2.452       | 0.026 | 2.373        | 0.028 |
| Precuneus                  | 2.274       | 0.027 | 2.294        | 0.026 |
| Rostral Anterior Cingulate | 2.683       | 0.045 | 2.822        | 0.049 |
| Rostral Middle Frontal     | 2.240       | 0.023 | 2.217        | 0.024 |
| Superior Frontal           | 2.496       | 0.025 | 2.468        | 0.025 |
| Superior Parietal          | 2.094       | 0.027 | 2.091        | 0.028 |
| Superior Temporal          | 2.640       | 0.032 | 2.641        | 0.031 |
| Supramarginal              | 2.396       | 0.026 | 2.390        | 0.027 |
| Frontal Pole               | 2.634       | 0.047 | 2.571        | 0.050 |
| Temporal Pole              | 3.560       | 0.067 | 3.647        | 0.068 |
| Transverse Temporal        | 2.273       | 0.042 | 2.298        | 0.046 |
| Insula                     | 2.816       | 0.035 | 2.810        | 0.036 |

Table B.3: Cortical thickness in MCI group (mean and standard deviation, millimeters)

| ROIs                       | MCI         |       |              |       |
|----------------------------|-------------|-------|--------------|-------|
|                            | <i>Left</i> |       | <i>Right</i> |       |
|                            | Mean        | S.D.  | Mean         | S.D.  |
| Bank of Superior Temporal  | 2.333       | 0.013 | 2.429        | 0.014 |
| Caudal Anterior Cingulate  | 2.579       | 0.022 | 2.445        | 0.021 |
| Caudal Middle Frontal      | 2.379       | 0.011 | 2.359        | 0.012 |
| Cuneus                     | 1.861       | 0.010 | 1.904        | 0.012 |
| Entorhinal                 | 3.158       | 0.031 | 3.236        | 0.035 |
| Fusiform                   | 2.610       | 0.013 | 2.642        | 0.014 |
| Inferior Parietal          | 2.263       | 0.012 | 2.298        | 0.012 |
| Inferior Temporal          | 2.646       | 0.015 | 2.672        | 0.013 |
| Isthmus Cingulate          | 2.256       | 0.016 | 2.300        | 0.018 |
| Lateral Occipital          | 2.139       | 0.011 | 2.195        | 0.011 |
| Lateral Orbital Frontal    | 2.513       | 0.012 | 2.488        | 0.012 |
| Lingual                    | 1.985       | 0.011 | 2.019        | 0.011 |
| Medial Orbital Frontal     | 2.309       | 0.013 | 2.319        | 0.013 |
| Middle Temporal            | 2.667       | 0.014 | 2.702        | 0.013 |
| Parahippocampal            | 2.704       | 0.025 | 2.651        | 0.021 |
| Paracentral                | 2.304       | 0.011 | 2.326        | 0.012 |
| Pars Opercularis           | 2.418       | 0.010 | 2.437        | 0.012 |
| Pars Orbitalis             | 2.548       | 0.015 | 2.532        | 0.014 |
| Pars Triangularis          | 2.296       | 0.011 | 2.307        | 0.012 |
| Pericalcarine              | 1.630       | 0.011 | 1.647        | 0.011 |
| Postcentral                | 2.003       | 0.010 | 1.993        | 0.010 |
| Posterior Cingulate        | 2.353       | 0.014 | 2.332        | 0.015 |
| Precentral                 | 2.446       | 0.011 | 2.407        | 0.012 |
| Precuneus                  | 2.231       | 0.011 | 2.262        | 0.011 |
| Rostral Anterior Cingulate | 2.653       | 0.019 | 2.811        | 0.021 |
| Rostral Middle Frontal     | 2.221       | 0.010 | 2.224        | 0.010 |
| Superior Frontal           | 2.479       | 0.011 | 2.478        | 0.011 |
| Superior Parietal          | 2.083       | 0.011 | 2.080        | 0.012 |
| Superior Temporal          | 2.557       | 0.013 | 2.576        | 0.013 |
| Supramarginal              | 2.359       | 0.011 | 2.370        | 0.011 |
| Frontal Pole               | 2.611       | 0.020 | 2.589        | 0.021 |
| Temporal Pole              | 3.422       | 0.028 | 3.486        | 0.029 |
| Transverse Temporal        | 2.231       | 0.018 | 2.268        | 0.019 |
| Insula                     | 2.793       | 0.015 | 2.794        | 0.015 |

Table B.4: Cortical thickness in AD group (mean and standard deviation, millimeters)

| ROIs                       | AD          |       |              |       |
|----------------------------|-------------|-------|--------------|-------|
|                            | <i>Left</i> |       | <i>Right</i> |       |
|                            | Mean        | S.D.  | Mean         | S.D.  |
| Bank of Superior Temporal  | 2.246       | 0.016 | 2.330        | 0.017 |
| Caudal Anterior Cingulate  | 2.618       | 0.027 | 2.455        | 0.025 |
| Caudal Middle Frontal      | 2.301       | 0.014 | 2.286        | 0.014 |
| Cuneus                     | 1.830       | 0.013 | 1.861        | 0.014 |
| Entorhinal                 | 2.759       | 0.038 | 2.890        | 0.043 |
| Fusiform                   | 2.502       | 0.016 | 2.535        | 0.017 |
| Inferior Parietal          | 2.165       | 0.015 | 2.201        | 0.015 |
| Inferior Temporal          | 2.523       | 0.018 | 2.564        | 0.016 |
| Isthmus Cingulate          | 2.157       | 0.020 | 2.204        | 0.021 |
| Lateral Occipital          | 2.075       | 0.013 | 2.147        | 0.014 |
| Lateral Orbital Frontal    | 2.511       | 0.014 | 2.494        | 0.014 |
| Lingual                    | 1.957       | 0.013 | 1.985        | 0.013 |
| Medial Orbital Frontal     | 2.282       | 0.015 | 2.325        | 0.016 |
| Middle Temporal            | 2.541       | 0.017 | 2.584        | 0.015 |
| Parahippocampal            | 2.528       | 0.030 | 2.510        | 0.026 |
| Paracentral                | 2.271       | 0.014 | 2.301        | 0.015 |
| Pars Opercularis           | 2.417       | 0.013 | 2.398        | 0.015 |
| Pars Orbitalis             | 2.558       | 0.018 | 2.555        | 0.018 |
| Pars Triangularis          | 2.283       | 0.014 | 2.315        | 0.014 |
| Pericalcarine              | 1.612       | 0.014 | 1.623        | 0.014 |
| Postcentral                | 1.966       | 0.012 | 1.936        | 0.012 |
| Posterior Cingulate        | 2.289       | 0.017 | 2.299        | 0.018 |
| Precentral                 | 2.403       | 0.013 | 2.381        | 0.014 |
| Precuneus                  | 2.133       | 0.014 | 2.159        | 0.013 |
| Rostral Anterior Cingulate | 2.630       | 0.023 | 2.819        | 0.025 |
| Rostral Middle Frontal     | 2.202       | 0.012 | 2.206        | 0.012 |
| Superior Frontal           | 2.426       | 0.013 | 2.433        | 0.013 |
| Superior Parietal          | 2.012       | 0.014 | 2.006        | 0.014 |
| Superior Temporal          | 2.449       | 0.016 | 2.495        | 0.016 |
| Supramarginal              | 2.280       | 0.013 | 2.303        | 0.014 |
| Frontal Pole               | 2.632       | 0.024 | 2.686        | 0.025 |
| Temporal Pole              | 3.246       | 0.034 | 3.298        | 0.035 |
| Transverse Temporal        | 2.228       | 0.021 | 2.241        | 0.024 |
| Insula                     | 2.718       | 0.018 | 2.732        | 0.018 |